



Cite this: *Nanoscale*, 2026, **18**, 66

## Overcoming barriers: nanomedicine-based strategies for nose-to-brain delivery

West Kristian Paraiso, <sup>\*a,b</sup> Carlos Palacín Ramos, <sup>a</sup> Parisa Mishal Hossain, <sup>b,c</sup> Carla Alvarez Gordi, <sup>a,b</sup> Pablo Adrian Guillen-Poza, <sup>d</sup> Sebastián Zagmunt, <sup>a</sup> Sabina Quader <sup>\*b</sup> and Rosalía Rodríguez-Rodríguez <sup>\*a,e</sup>

For therapeutics to reach the brain, the several administration routes available come with some disadvantages, with the primary biological obstacle being the blood–brain barrier (BBB), which is not easy to penetrate despite the sophisticated technologies which have been developed. In addition, reaching specific brain structures invokes additional challenges, entailing more complicated delivery strategies. Nose-to-brain (N2B) delivery or the intranasal (IN) administration route provides a less invasive alternative. With the wealth of knowledge available on N2B delivery of nanomedicines and biotherapeutics, there is an opportunity to synthesize the current literature, especially in terms of promising strategies to improve N2B delivery of nanomedicines, highlighting experimental evaluation and translational challenges. We also emphasized the latest advancements in experimental models for nasal delivery. Aiming to bridge the gap between bench research and clinical application, we reviewed the cases of insulin and oxytocin, two biotherapeutics with high clinical potential for CNS-related diseases, and explore how nanomedicine-based platforms can enhance their effectiveness. This review offers a roadmap for overcoming barriers and accelerating the clinical translation of N2B therapeutics.

Received 28th May 2025,  
Accepted 16th November 2025

DOI: 10.1039/d5nr02259b  
[rsc.li/nanoscale](http://rsc.li/nanoscale)

### Introduction to intranasal pathways

Intranasal (IN) administration has emerged as an attractive, non-invasive route for drug delivery, offering distinct advantages over conventional systemic administration.<sup>1</sup> By bypassing the gastrointestinal tract and hepatic first-pass metabolism, IN delivery enables faster therapeutic onset, improved patient compliance, and reduced systemic side effects.<sup>1–4</sup> More recently, this route has also been explored for nanoparticle-based formulations, which offer the potential for precise and targeted delivery to brain cells, with important translational and clinical applications in neuroscience.

Traditional administration routes, such as oral and intravenous, present multiple hurdles for central nervous system (CNS) therapeutics, including poor bioavailability (BA), systemic toxicity, and the challenge of delivering sufficient con-

centrations to the brain.<sup>1</sup> Chief among these barriers is the blood–brain barrier (BBB), a tightly regulated interface that prevents most therapeutic molecules from entering the brain. Additional challenges include off-target distribution, enzymatic degradation, and the need for high systemic doses that may exacerbate side effects.<sup>1</sup>

In contrast, IN administration provides direct access to the CNS through two distinct pathways<sup>5</sup> (Fig. 1). The indirect pathway involves absorption into nasal vasculature, followed by systemic circulation and subsequent crossing of the BBB, a route that largely resembles conventional systemic delivery and thus remains suboptimal.<sup>6,7</sup> More importantly, the direct pathway exploits the anatomical connection of the olfactory and trigeminal nerves to the brain, allowing drugs to bypass the BBB and reach the CNS more efficiently. This direct transport minimizes systemic exposure, reduces the risk of peripheral toxicity, and enables localized and rapid therapeutic action.<sup>3,4</sup> These features make the IN route particularly appealing for a wide range of therapeutic modalities, including small molecules, peptides, proteins, and nanomedicines.

Beyond pharmacokinetic advantages, IN delivery is non-invasive, patient-friendly, and suitable for self-administration,<sup>4</sup> making it particularly beneficial for home care, vulnerable patients who may experience difficulties with other routes of administration, or for those requiring emergency interventions.<sup>8,9</sup> Clinical studies further highlight its accept-

<sup>a</sup>Department of Biomedical Sciences, Faculty of Medicine and Health Sciences, Universitat Internacional de Catalunya (UIC), Sant Cugat del Vallès, 08195, Spain. E-mail: [wkparaiso@uic.es](mailto:wkparaiso@uic.es), [rrodriguez@uic.es](mailto:rrodriguez@uic.es)

<sup>b</sup>Innovation Center of Nanomedicine, Kawasaki Institute of Industrial Promotion, Kawasaki, Kanagawa 210-0821, Japan. E-mail: [sabina-q@kawasaki-net.ne.jp](mailto:sabina-q@kawasaki-net.ne.jp)

<sup>c</sup>Faculty of Health Sciences, McMaster University, Hamilton, Ontario, Canada

<sup>d</sup>School of Biomedical Sciences, Li Ka Shing Faculty of Medicine, The University of Hong Kong, Hong Kong SAR

<sup>e</sup>Centro de Investigación Biomédica en Red de Fisiopatología de la Obesidad y la Nutrición (CIBEROBN), Instituto de Salud Carlos III, Madrid, 28029, Spain



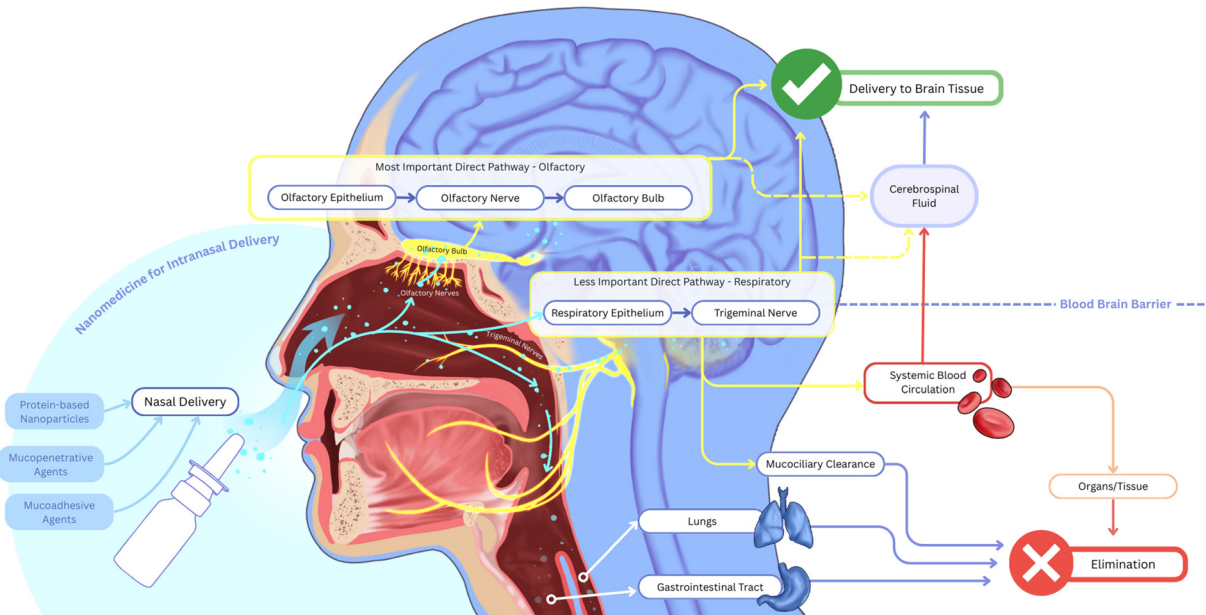


**Fig. 1** Schematic overview of intranasal deposition and transport routes showing primary direct transport via olfactory epithelium, to olfactory nerve, to olfactory bulb and secondary direct transport via respiratory epithelium to trigeminal nerve, enabling nanoparticle delivery to the cerebrospinal fluid (CSF) and brain tissue while bypassing the blood brain barrier (BBB). Off-target clearance and systemic distribution: mucociliary clearance to lungs and gastrointestinal tract, systemic absorption into systemic blood circulation, and eventual elimination are also illustrated. Adapted from reference [S. Nakhaee, F. Saeedi and O. Mehrpour, *Helijon*, <https://doi.org/10.1016/j.heliyon.2023.e23083>], used under Creative Commons Attribution-International License 4.0 (CC BY).

ability and feasibility, especially in conditions where rapid CNS drug action is required.<sup>10,11</sup>

Nevertheless, nose-to-brain (N2B) delivery faces critical challenges. The nasal cavity is equipped with enzymatic activity that can degrade therapeutic molecules, resulting in low BA.<sup>12,13</sup> The mucus layer and mucociliary clearance further hinder residence time and penetration of nanoparticles. Moreover, cellular barriers such as tight junctions and plasma membranes complicate para- and transcellular transport, limiting delivery efficacy.<sup>13,14</sup> These obstacles underscore the need for advanced formulation strategies that can improve stability, retention, and brain penetration of IN- administered therapeutics.

Nanomedicine offers powerful solutions to overcome these limitations. Polymeric micelles, liposomes, protein- and cell-based nanoparticles, and other advanced systems can enhance drug stability, improve bioavailability, and provide controlled release while reducing off-target effects. By modulating size, surface charge, and surface functionalization, nanomedicines can be engineered to reduce mucosal clearance, penetrate mucus barriers, and protect drugs from enzymatic degradation. Emerging approaches include mucoadhesive and mucopenetrative agents, mucus-modifying systems, protein-based nanoparticles, and biomimetic nanomedicines.

In this review, we discuss recent and promising strategies to improve N2B delivery of nanomedicines, highlighting experimental evaluation and translational challenges. We particularly emphasize the case of insulin and oxytocin, two biothera-

peutics with high clinical potential for CNS-related diseases and explore how nanomedicine-based platforms can enhance their effectiveness. By integrating advances in nanotechnology with translational insights, this review aims to provide a roadmap for overcoming current barriers and accelerating the clinical application of IN therapeutics.

## Pharmacokinetics and brain distribution of therapeutics following nose-to-brain delivery

### Anatomy of the intranasal pathway

The human nasal cavity, divided by the nasal septum, possesses a total volume of approximately 16 to 19 mL and an estimated surface area of around 180 cm<sup>2</sup>, with over 75 cm<sup>2</sup> suitable for drug absorption.<sup>15</sup> Upon IN administration, drugs navigate through three distinct anatomical areas: the vestibular (VR), respiratory (RR), and olfactory regions (OR). The VR, situated nearest to the nostrils, is the smallest and has a surface area of roughly 0.6 cm<sup>2</sup>, lined with stratified squamous epithelium and featuring vibrissae that serve as initial filters for inhaled particles, thus contributing minimally to drug absorption.<sup>16</sup> In contrast, the RR, which constitutes 80–90% of the nasal cavity surface area, consists of pseudostratified columnar ciliated epithelium, characterized by its rich vascularization and innervation, facilitating drug transport through perineuronal and perivascular pathways.<sup>15</sup>

Rodents exhibit notable anatomical distinctions in their nasal cavities, which are adapted for specific species needs while serving similar functions to those in humans. With nasal cavity volumes of approximately 257 mm<sup>3</sup> in rats and 32 mm<sup>3</sup> in mice, these dimensions afford large relative nasal surface areas compared to body size, making rodents advantageous for N2B delivery research.<sup>17,18</sup> The rodent nasal cavity includes a nasal vestibule lined with squamous epithelium and vibrissae, a respiratory region (RR) featuring ciliated epithelium, and an olfactory region (OR). A key anatomical difference is the pronounced vomeronasal organ, which specializes in pheromone recognition. Furthermore, the nasopharynx connects the nasal cavity to the pharynx, allowing for airway passage, which ultimately underscores the structural variations in both humans and rodents that critically influence the efficacy of nasal drug delivery.<sup>19</sup>

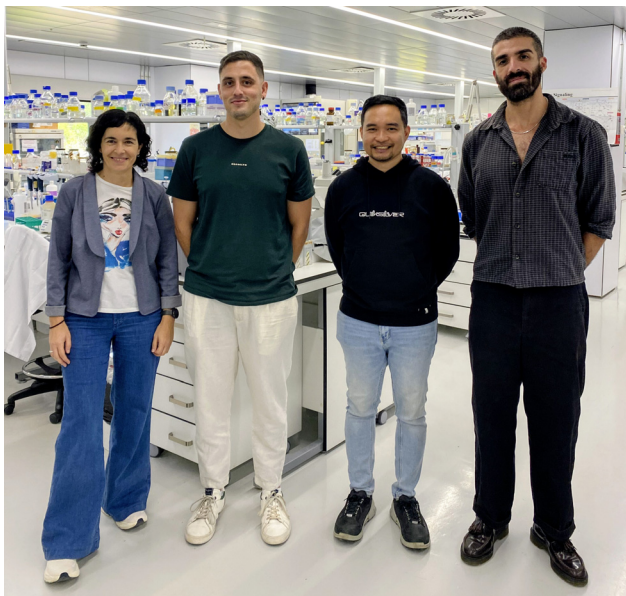
The OR is rich in sensory cells and contains olfactory nerves that originate from specialized cells in the olfactory epithelium, located at the roof of the nasal cavity. These nerves extend to the olfactory bulb, an essential structure in the brain responsible for processing smells. Both the olfactory and trigeminal nerves can absorb high drug concentrations from the nasal cavity and transport them to reach the brain or other related structures.<sup>20</sup> This was previously described as the direct pathway, which is ideal for N2B delivery. Here, drugs that are delivered through the olfactory nerve pathway travel through the olfactory epithelium, anterior olfactory nucleus, olfactory tract, amygdala, hypothalamus, and piriform cortex. The olfactory receptor neurons (ORNs) are responsible for the transduction of substances. The cilia located on these cells

conduct the transduction. Molecules can reach the ORNs *via* two different transcellular (across the cell membrane) or paracellular (between the cells) mechanisms. Due to tight junctions, many molecules are absorbed by paracellular mechanisms, taking only a few minutes to reach the CNS. Another mechanism is *via* transcellular transport through the olfactory and trigeminal nerves (Fig. 1). This axonal transport can transfer the substances to the olfactory bulb or cerebrospinal fluid (CSF). However, several hours to days are needed for the transportation of drugs to the brain.<sup>6,7</sup>

Additionally, drugs delivered through the trigeminal nerve can reach the pons and cerebellum, which are parts of the hindbrain. The trigeminal nerve begins at the pons and extends into the nasal cavity. Some drugs that enter the RR can also be transported directly to the brain *via* the trigeminal nerve pathway, utilizing either transcellular or paracellular routes.<sup>20</sup>

#### Pharmacokinetics and brain distribution of small molecules administered *via* nose-to-brain delivery

Pérez-Osorio *et al.* (2021) studied the brain biodistribution of dexamethasone administered IN *versus* IV. Their experiments demonstrated that higher concentrations of dexamethasone were present in all regions of the brains of mice that received the administration. HPLC analysis further indicated that N2B delivery allows dexamethasone to reach the brain more quickly and in greater concentrations compared to IV, with the quantification being corroborated by immunofluorescence. These results support the use of IN dexamethasone as a more effective alternative for controlling neuroinflammation.<sup>21</sup>



**Left to right: Dr Rosalia Rodríguez-Rodríguez, Carlos Palacín Ramos, Dr West Kristian Paraiso, and Dr Sebastián Zagmunt.**

The NeuroNanoMet Group, led by Dr Rosalia Rodríguez-Rodríguez, Professor in Pharmacology at the Universitat

Internacional de Catalunya (UIC Barcelona), is part of the Department of Biomedical Sciences, Faculty of Medicine and Health Sciences in the Sant Cugat Campus. The group employs interdisciplinary approaches that combine molecular biology and nanotechnology to investigate neuro-glial metabolism and signaling in the hypothalamus, and their roles in metabolic disorders such as obesity and diabetes. Their work explores novel nanomedicine-based therapeutic strategies for these conditions.

Carlos Palacín Ramos, predoctoral researcher in neurometabolism, develops intranasal protein-based nanoparticles for obesity therapy. Dr West Kristian Paraiso, pharmacist and Beatriu de Pinós fellow, designs polymeric micelles as drug delivery systems for cancer and CNS diseases. Dr Sebastián Zagmunt, neuroscientist and group co-leader, focuses on neuroinflammation and the role of hypothalamic targets in food intake and energy homeostasis.

The NeuroNanoMet Group maintains collaborations with local and international partners – the University of Barcelona, the Institut de Biotecnología i de Biomedicina (Autonomous University of Barcelona), the Innovation Center of Nanomedicine (iCONN, Japan), and the University of Catania (Italy) – advancing nanomedicine research across disciplines.



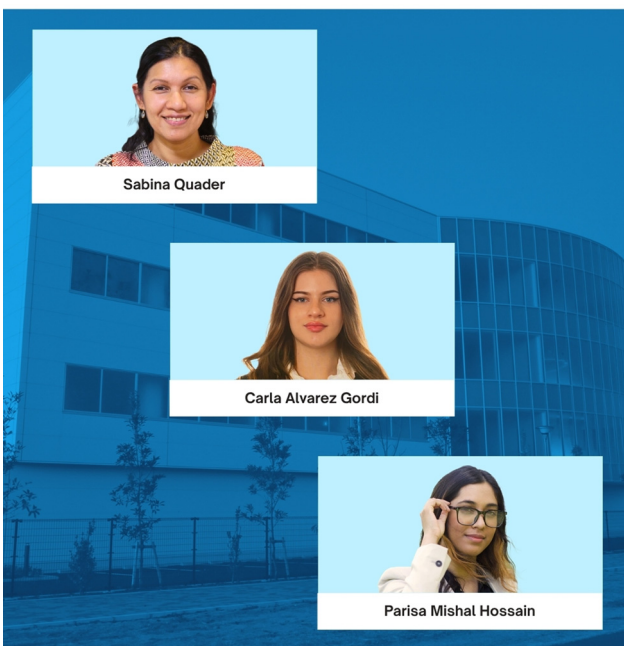
In another study by Banks *et al.* (2009), the effects of IN *versus* IV administration of tritiated testosterone (3H-T) were compared. They found that about 75% of 3H-T given by IN entered the bloodstream, however, whole brain levels of 3H-T were approximately twice as high compared to IV. Approximately two-thirds of the testosterone that reached the brain *via* IN administration did so directly through the nasal pathways, while the rest entered the bloodstream first (indirect pathway). Most brain regions, except the frontal cortex, showed higher testosterone levels after IN administration, particularly in the olfactory bulb, hypothalamus, striatum, and hippocampus. The study indicated that testosterone distribution likely involves various routes, including CSF and nerve projections. Overall, both routes showed similar regional distribution patterns, suggesting a common factor influences how testosterone is distributed and retained. The researchers concluded that IN administration specifically targets brain regions such as the olfactory bulb, hypothalamus, striatum, and hippocampus.<sup>22</sup>

The IN route also outperforms intraperitoneal (IP) administration in delivering therapeutics to the mouse brain. In another study, researchers compared time-dependent uptake and retention of various radiolabelled neurotherapeutics administered either IN or IP. The findings revealed that the brain uptake of IN-delivered therapeutics was over five times greater than that achieved using IP. The peak uptake and

retention time for all IN therapeutics across different brain regions was observed to range from 30 minutes to 12 hours. This variation depended on the distance of the brain region from the administration site. Gradually, the radioactive counts declined by 24 hours following administration. This study confirms the effectiveness of IN administration as a non-invasive and efficient method for CNS delivery, particularly for treating neurodegenerative diseases, including Alzheimer's disease (AD).<sup>23</sup>

#### Pharmacokinetics and brain distribution of macromolecules administered *via* nose-to-brain delivery

In addition to small molecule therapeutics, macromolecules or macromolecular drug delivery systems (DDS) can also be effectively delivered to the brain by IN route. Yadav *et al.* (2015) conducted a study on the biodistribution and PK of cyclosporine A (CsA) following IN and IV administration in Sprague-Dawley rats. They used an oil-in-water nanoemulsion (CsA-NE) and compared the results with an aqueous solution of CsA (CsA-A) that contained phosphatidylcholine, Tween 80, and stearylamine. CsA is a hydrophobic immunosuppressive peptide known for its anti-neuroinflammatory and neuroprotective effects. Here, both the CsA-NE and CsA-S were prepared using ultrasonication. The findings revealed that IN-administered CsA-NE resulted in the highest levels of brain accumulation compared to other routes and treatments across all eval-



KAWASAKI INSTITUTE OF INDUSTRIAL PROMOTION  
Innovation Center of NanoMedicine

Left to Right: Dr Sabina Quader, Carla Alvarez Gordi, Parisa Mishal Hossain.

*The Nanomedicine Group at the Innovation Center of NanoMedicine (iCONM) in Kawasaki, Japan, is led by Dr Sabina Quader, Deputy Principal Research Scientist. iCONM is a world-class research hub that bridges academia, industry, and medicine to accelerate the translation of nanotechnology into clinical applications. It fosters a highly collaborative environment, hosting numerous local and international partnerships to advance the field of nanomedicine.*

*Under Dr Quader's leadership, the group focuses on developing multifunctional nanomaterials for targeted drug delivery, with an emphasis on disorders of the central nervous system, most especially brain cancer. Her research aims to overcome biological barriers and improve therapeutic precision through innovative polymeric micelle systems. As Chief Coordinator of Global Partnerships, she also oversees international research collaborations and internship programs, promoting global scientific exchange and nurturing young researchers.*

*Current team members include Carla Alvarez Gordi, a Biomedical Science graduate from UIC Barcelona, conducting characterization studies on polymeric micelles in neuroinflammatory models, and Parisa Mishal Hossain, a Health Sciences undergraduate from McMaster University, who contributed to imaging-focused micelle design during her 2023 internship.*

*Together, the group exemplifies iCONM's mission to integrate innovation, collaboration, and education in advancing next-generation nanomedicine.*



uated regions, including the olfactory bulbs, midbrain, and hindbrain. The brain-to-blood exposure ratio for CsA-NE (IN) was 4.49, which is approximately 450 times higher than that of the IV route, indicating effective N2B transport (Fig. 2). Moreover, CsA-NE led to approximately a 14-fold improvement in brain exposure compared to CsA-S, highlighting the advantages of nanomedicine formulation. Additionally, CsA-NE reduced exposure of non-target organs. These findings suggest that nasal CsA-NE is a promising strategy for enhancing brain targeting while minimizing peripheral exposure and potential off-target toxicity.<sup>24</sup>

In another study, dye-labelled mesenchymal stromal cell-derived extracellular vesicles (MSC-EVs) were administered to BALB/c mice *via* IV, intratracheal (IT), and IN routes. Distribution was monitored immediately and at 3- and 24-hours post-injection.<sup>25</sup> After 3 hours, IV injection showed accumulation of MSC-EVs in the abdominal region, IT localized them in the chest, while IN distributed them in the brain. After 24 hours, the same areas showed a stronger signal; isolated organ analysis confirmed significant EV accumulation in the spleen and liver after IV administration. For IT, a stronger signal was found in the lungs, but for IN, it remained confined to the brain.

The results of the PK and brain biodistribution studies presented above indicate that the IN route generally outperforms the IV, IP, and IT routes in terms of delivering substances to the brain while also reducing systemic exposure. This presents a unique advantage for IN administration, as it is a non-invasive method. However, it is important to note that all these studies have been conducted in small animals, so further validation in larger animals is necessary before progressing to human trials.

*Dr Pablo Adrián Guillén Poza earned a Life Sciences Ph.D. from Hokkaido University, Japan, supported by the MEXT Scholarship. After a postdoctoral stint and a tenure as Assistant Professor under Prof. Dr Katsumi Maenaka—specializing in solid-phase peptide synthesis and drug discovery—he moved to The University of Hong Kong. There, he currently serves as a Postdoctoral Fellow. His research centers on structural biology, employing Cryo-EM to investigate pathological and functional amyloids. The work aims to illuminate amyloid structure–function relationships and advance understanding of their roles in disease, with broader implications for therapeutic targeting and biomolecular design.*

**Pablo Adrian Guillen-Poza.**

*employing Cryo-EM to investigate pathological and functional amyloids. The work aims to illuminate amyloid structure–function relationships and advance understanding of their roles in disease, with broader implications for therapeutic targeting and biomolecular design.*

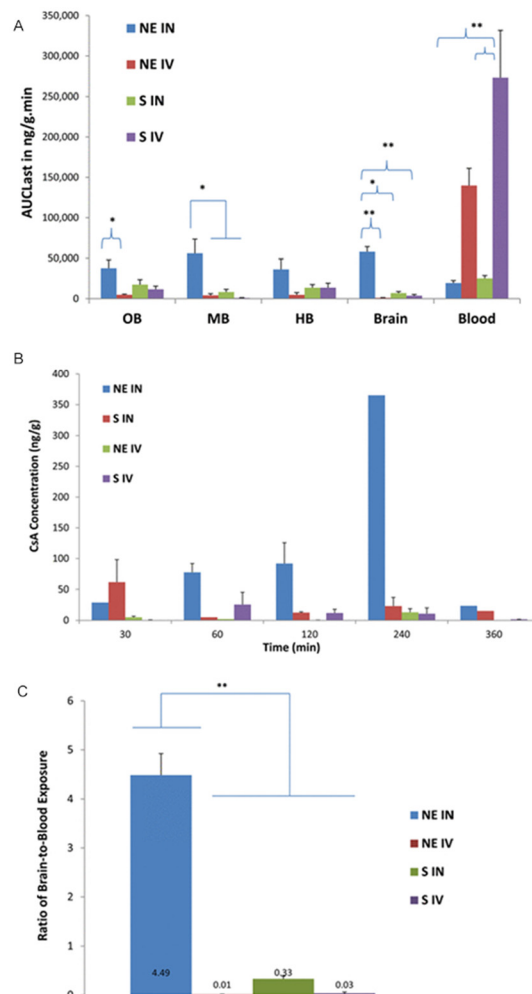


**Fig. 2** (A) Area-under-the-curve (AUC) values calculated from mean cyclosporine-A (CsA) concentration in blood and different regions of brain after administration of CsA-nanoemulsion (CsA-NE) or CsA-solution (CsA-S) *via* the intranasal (IN) or intravenous (IV) route. OB, olfactory bulb; MB, mid brain; HB, hind brain. (B) Mean  $\text{ng g}^{-1}$  brain concentration–time plot of CsA in rats after IN or IV administration of CsA-NE or CsA-S at a dose of  $5 \text{ mg kg}^{-1}$ . (C) Comparison of brain targeting efficiency of IN and IV routes of delivery for both CsA-NE and CsA-S. \* $p < 0.05$  or \*\* $p < 0.01$  compared to various control groups. Reprinted with permission from reference [M. B. Chauhan and N. B. Chauhan, *J. Neurol. Neurosurg.*, 2015, 2, 009]. Copyright American Chemical Society 2015.

## Strategies in improving nose-to-brain delivery

As mentioned earlier, N2B delivery of therapeutics provides enhanced effectiveness by bypassing systemic exposure in comparison to other administration methods. Nevertheless, utilizing this route remains difficult due to several barriers, most notably the rapid mucociliary clearance system and enzymatic degradation in the nasal cavity. Physicochemical properties and compositional characteristics of molecules play a significant role in their ability to withstand these barriers and ultimately determine their fate within the different pathways



leading to the brain and CSF.<sup>26</sup> Nanomedicines address several key challenges in drug delivery and imaging. They enhance drug efficiency, minimize adverse effects by limiting non-specific tissue distribution, improve BA, and enable precise control over the release of therapeutic or imaging agents.<sup>27</sup> Importantly, these systems can be tailored to overcome the specific limitations of IN delivery. By prolonging retention at the nasal mucosa or facilitating penetration across mucus, and by shielding drugs from enzymatic degradation through protective coatings or encapsulation, nanomedicines hold tremendous potential to transform drug distribution *via* N2B delivery.<sup>28</sup>

### The role of mucus in intranasal delivery

The mucus layer of the nasal mucosa serves as a critical component of the innate defense system, protecting against pathogens and foreign particles while simultaneously regulating hydration and ciliary function. However, it also represents a major obstacle for IN formulations. Composed mainly of water (95–99%) and mucins (large, glycosylated proteins secreted by goblet cells) respiratory mucus exhibits a biphasic gel structure that supports mucociliary clearance by trapping particles and facilitating their removal.<sup>29,30</sup> The mucin network, with its mesh-like structure and nanoscale pores, acts as a size-selective filter, meaning that DDS designed for effective diffusion should be nano-sized. Nevertheless, particle size alone is insufficient to guarantee diffusion: rheological properties and particle dynamics also strongly influence mucus permeability. Studies indicate that rod-shaped nanoparticles penetrate more effectively than spherical ones.<sup>31</sup> Similarly, surface charge is critical, as mucins carry a net negative charge. Positively charged carriers often adhere strongly and are cleared more rapidly, whereas neutral or negatively charged particles exhibit greater mobility through the mucus matrix.<sup>32</sup> Surface modifications such as PEGylation not only reduce adhesive interactions but also provide a protective shield against enzymatic attack, thereby enhancing both diffusion and stability.

To counteract these limitations, two complementary design philosophies are widely explored. Mucopenetrative nanoparticles are engineered to minimize interactions with the mucus layer and reduce enzymatic exposure. By coating carriers with hydrophilic polymers such as poly(ethyleneglycol) (PEG), nanoparticles acquire neutral and hydrophilic surface characteristics that prevent strong adhesion with mucins while also shielding encapsulated drugs from enzymatic degradation, further increasing their BA. Their small size facilitates transcellular transport and rapid diffusion across the mucus gel into deeper tissues, ultimately granting faster access to the olfactory region and brain.<sup>33,34</sup>

Such designs are particularly useful when rapid and efficient CNS delivery is required. For instance, Date *et al.* (2018) showed that PEG-poly(lactic-co-glycolic acid) nanoparticles exhibited significantly greater penetration and translocation capabilities compared to mucoadhesive systems, underlining the crucial role of surface modification for mucopenetration.<sup>35</sup>

Mucoadhesive nanoparticles, by contrast, exploit interactions with the mucus to prolong residence time in the nasal cavity, thereby counteracting the rapid mucociliary clearance mechanism. The adhesion achieved through electrostatic forces, hydrogen bonding, or mechanical entrapment slows clearance and increases the opportunity for absorption across epithelial barriers. Polymers such as chitosan and Carbopol are well-studied in this regard, not only enhancing contact time but also providing a degree of protection against enzymatic degradation by retaining the formulation at the absorption site.<sup>36–38</sup> Pathak *et al.* (2014) reported that formulations using surfactants combined with mucoadhesive polymers significantly improved the N2B delivery of nimodipine while sodium hyaluronate has also been shown to enhance retention and delivery efficiency.<sup>36,39,40</sup>

Overall, both approaches directly address the primary barriers of IN delivery, rapid mucociliary clearance and enzymatic degradation, but through opposite mechanisms. Mucopenetrative systems focus on evading mucus entrapment and enzymatic contact, while mucoadhesive systems resist clearance by prolonging residence time and stabilizing the formulation. The choice between them depends on the therapeutic goal, drug stability, and required kinetics of brain delivery. By carefully tuning particle size, shape, surface charge, and functional coatings, nanomedicine platforms provide versatile solutions to overcome these challenges and enhance the efficiency of N2B delivery.<sup>41</sup>

### Mucoadhesive agents

**Chitosan.** The cationic polysaccharide chitosan serves as an effective excipient for nasal delivery, enhancing drug absorption through mucoadhesion and permeation enhancement by loosening tight junctions in the nasal epithelium.<sup>42</sup> A key application is in improving the CNS delivery of quetiapine hemifumarate (QF), which faces challenges due to its poor solubility and low oral BA. Gadhave *et al.* (2024) developed biodegradable PLGA NPs loaded with QF, incorporating surface charge modifications using poloxamer and chitosan, to enhance brain targeting and nasal epithelium transport in RPMI-2650 cells. The researchers prepared a QF-loaded poloxamer 407-chitosan-PLGA *in situ* gel (QF-PLGA-ISG) which not only improved cellular uptake but also increased QF transport across the epithelial monolayer by 1.5 to 2 times. Additionally, experiments using the EpiNasal<sup>TM</sup> 3D nasal tissue model confirmed the safety and efficacy of the QF-PLGA-ISG formulation, achieving up to a fourfold increase in transport compared to plain QF after four hours.<sup>43</sup>

Interferon (IFN)- $\beta$  is a first-line treatment for multiple sclerosis (MS) but its effectiveness is limited by the need for injectable administration, a short half-life, and restricted CNS access.<sup>44</sup> González *et al.* (2021) developed IFN- $\beta$ -loaded chitosan and sulfobutylether- $\beta$ -cyclodextrin nanoparticles (IFN- $\beta$ -NPs) for N2B delivery. Following the administration of fluorescent probe-loaded nanoparticles, significant fluorescence signals were detected in mice brains. In a mouse model of



experimental autoimmune encephalomyelitis (EAE), IFN- $\beta$ -NPs led to notable improvements in clinical symptoms, while a similar dose of free IFN- $\beta$  (either IN or systemic). Additionally, spinal cords from EAE mice treated with IFN- $\beta$ -NPs exhibited fewer inflammatory foci and demyelination, reduced expression of antigen-presenting and costimulatory proteins on CD11b $^{+}$  cells, and decreased activation of astrocytes and microglia compared to controls.<sup>45</sup>

Discoidal high-density lipoproteins (HDL-Disc) can be used to mimic amyloid  $\beta$ -peptide (A $\beta$ ) antibodies to influence directional flux of A $\beta$  from central to peripheral catabolism as a strategy to treat AD.<sup>46</sup> Zhang *et al.* (2023) prepared HDL-Disc (polyDisc) *via* chitosan derivative polymerization (CP50k and CP150k molecular weight to make poly<sub>50</sub>Disc and poly<sub>150</sub>Disc, respectively). When administered IN, the acidic nasal environment breaks it down into HDL-Disc and chitosan derivatives that transiently open tight junctions, allowing the HDL-Disc to enter the brain *via* the OR. The transport of HDL-Disc was evaluated using ELISA in blood and key organs, including the olfactory bulb, brain, liver, and lung. After IN administration, HDL-Disc particles were detected more abundantly in the olfactory bulb and brain of AD mice within 15 minutes, indicating the olfactory pathway supports rapid brain transport. The analysis showed that the percentage of injected dose per gram of brain tissue (% ID g<sup>-1</sup>) in the poly<sub>150</sub>Disc group was 2.47-fold and 3.28-fold higher than in the poly<sub>50</sub>Disc and free HDL-Disc groups, respectively, signifying effective brain accumulation following nasal delivery with poly<sub>150</sub>Disc. Differences in HDL-Disc accumulation based on chitosan density were observed in the brain and liver. Overall, these results suggest that the CP150k polymer enhances HDL-Disc mucoadhesion and facilitates its distribution to the brain and liver for A $\beta$  catabolism. The transport pathway for polyDisc can thus be summarized as nose  $\rightarrow$  brain  $\rightarrow$  liver, with CP150k being particularly effective for nasal penetration in AD treatment. Upon reaching the brain, the HDL-Disc removes A $\beta$  through microglia or transports it for liver degradation. In APPswe/PS1dE9 AD mice, this approach significantly reduces both intracerebral and vascular A $\beta$ , improving neurological function and memory.<sup>46</sup>

**Cellulose derivatives.** IN delivery of phenytoin may offer a novel method to enhance its safety and effectiveness in treating status epilepticus. To overcome its low water solubility, the hydrophilic prodrug fosphenytoin was utilized in straightforward aqueous IN formulations. Pires *et al.* (2021) demonstrated that phosphate ester prodrugs can effectively improve the N2B delivery of poorly soluble drugs like phenytoin. A formulation combining hydroxypropyl methylcellulose (HPMC) and albumin extended the drug concentration in the brain over time, resulting in increased absolute BA. This formulation also contained a small quantity of the active lipophilic form, which was prepared as a nanoemulsion, further elevating and prolonging drug levels. Only phenytoin was detected in both the brains and blood of mice, indicating that fosphenytoin was rapidly converted to phenytoin, either within the nasal cavity or following absorption.<sup>47</sup>

Edaravone is a potent antioxidant drug approved for treating amyotrophic lateral sclerosis (ALS), but its short biological

half-life and poor water solubility require hospitalization for IV infusion. PLGA-based nanoparticles loaded with edaravone effectively reduced hydrogen peroxide-induced oxidative stress in the BV-2 mouse microglial cell line. For IN delivery, a 200  $\mu$ L pipette was used to instil 10  $\mu$ L into each nostril under inhalation anesthesia, with the nanoparticles suspended in 0.5% carboxymethylcellulose (CMC) in saline to enhance mucosal contact. Optical imaging revealed that N2B delivery in CD-1 mice resulted in higher and more sustained brain uptake of edaravone compared to IV administration. Additionally, ultra-performance liquid chromatography-tandem mass spectrometry (UPLC-MS/MS) confirmed that the injected dose per gram of brain tissue in Kunming mice was highest (approximately 0.8%) compared to the IV administered free drug.<sup>48</sup>

**Poloxamer.** Michaels *et al.* (2023) developed a lipid nanoemulsion incorporating the thermoresponsive polymer Poloxamer 407 to enhance the release of temozolomide (TMZ). They assessed the effects of varying polymer concentrations (2.5% to 12.5%) and temperature on viscosity, along with their impact on mucoadhesion, TMZ release rate, and retention or permeation through porcine nasal mucosa using Franz-type diffusion cells. At a concentration of 10% poloxamer 407, a significantly greater amount of TMZ was detected in rat brains, along with a notable reduction in tumor growth compared to control groups.<sup>49</sup>

**Carbopol.** A D- $\alpha$  tocopheryl PEG<sub>1000</sub> succinate (TPGS)-based mucoadhesive nanoemulsion (ARP-MNE) was developed for N2B delivery of aripiprazole to treat schizophrenia. TPGS, a vitamin E derivative, enhanced drug mucosal permeability. The nanoemulsion also incorporated Carbopol 971, a mucoadhesive polymer, which improved *ex vivo* permeation through sheep mucous membranes without causing ciliotoxicity. In Wistar rats, ARP-MNE achieved a higher maximum concentration in the brain ( $C_{max}$ ) compared to non-mucoadhesive formulations. It also demonstrated high drug targeting efficiency (96.9%) and drug targeting potential (89.73%). Notably, treated rats exhibited no extrapyramidal symptoms in catalepsy and forelimb retraction tests, confirming the antipsychotic efficacy of ARP-MNE.<sup>50</sup>

**Ion-pair complexes.** Subhash-Hinge *et al.* (2023) studied the effect of rivastigmine-containing lipid polymeric hybrid (LPH) nanoparticle charge on its N2B delivery. Rivastigmine hydrogen tartrate (RIV-HT) poses difficulties due to its hydrophobicity, which limits absorption in the nasal cavity and complicates nanoparticle encapsulation. A potential solution is to develop hydrophobic ion pair complexes (IPC) to enhance N2B delivery. These hydrophobic IPCs can increase lipophilicity without changing the drug's chemical structure, allowing for reversible aqueous solubility of the hydrophilic drug. In this study, they combined RIV-HT with docosahexaenoic acid (DHA) to form ion-pair complexes (RIV : DHA), which they then loaded into cationic and anionic LPH nanoparticles. The resulting thermoresponsive gel containing LPH nanoparticles improved nasal drug retention. Cationic LPH nanoparticles demonstrated significantly better PK parameters compared to their anionic counterparts, resulting in higher brain concentrations. Histological analysis of the nasal mucosa treated confirmed the biocompatibility of the delivery system.<sup>51</sup>



## Mucopenetrative agents

**Polyethylene glycol and end-group functionality effect.** Kurano *et al.* (2022) examined how the surface properties of nanomedicines affect nasal cavity to brain transport. They created fluorescently- and radioactively-labelled liposomes with different surface charges (positive, neutral, and negative) and some PEG modifications (with or without), all under 100 nm in size. The distribution of these liposomes in the CNS was analyzed using *ex vivo* imaging, with administration *via* an esophageal reverse-intubation method for consistent PK assessment.<sup>52</sup>

Qualitative analysis showed that neutral PEGylated liposomes distributed widely in the brain and spinal cord within 60 minutes, while non-PEGylated neutral liposomes localized in the olfactory bulb. Positively charged liposomes had low fluorescence in the brain and spinal cord, with stronger signals in the olfactory bulb (OB) after 120 minutes. Negatively charged liposomes initially showed no fluorescence but displayed low levels throughout the brain and spinal cord after 120 minutes.<sup>52</sup> Quantitative results using radioactivity confirmed that neutral liposomes had the highest brain and spinal cord distribution, with positively charged liposomes more prevalent in the OB and forebrain and negatively charged liposomes more concentrated in the hindbrain. PEGylated neutral liposomes showed significantly enhanced distribution compared to non-PEG-modified ones after 90 minutes. These findings highlight the importance of surface charge and PEG modification in enhancing N2B delivery efficiency, with PEG-modified neutral liposomes being particularly effective for broad CNS delivery.<sup>52</sup>

**Cyclodextrin and borneol as permeability enhancers.** A nasal delivery system was developed using borneol (BO)-modified cyclodextrin-metal organic framework (BO-CDF) in a cubic shape as a drug carrier to improve the permeation of rivastigmine and enhance its targeting to the brain. The BO-CDF formulation increased mucoadhesion and significantly enhanced rivastigmine permeability, resulting in plasma AUC values, brain AUC, and  $C_{\max}$  values that were 1.7, 2.3, and 8 times greater, respectively, compared to those observed with PO rivastigmine solution in rats.<sup>53</sup>

For AD treatment, a cyclodextrin-based metal-organic framework (CD-MOF) was utilized to load huperzine A effectively. These potassium-structured CD-MOFs, enhanced with stigmasterol and lactoferrin, exhibited improved stability and biocompatibility. The formulation was delivered *via* a toothbrush-like microneedle patch made of hyaluronic acid microneedles and gelatin crosslinked with tannic acid, which dissolved rapidly in the nasal mucosa to release the CD-MOFs. Following N2B delivery in Sprague-Dawley rats, the treatment significantly reduced neurocyte damage caused by hydrogen peroxide and scopolamine. Huperzine A's effectiveness against memory deficits induced by scopolamine and D-galactose and aluminum chloride was notably enhanced, as shown by reduced acetylcholinesterase activity, decreased oxidative stress in the brain, and improved learning functions.<sup>54</sup>

**Cell-penetrating peptides (CPPs).** Also known as protein transduction domains (PTDs), CPPs are versatile tools in bio-

medical research, allowing the transport of different payloads into cells through various mechanisms. CPPs are 5–40 amino acids-long cationic peptides naturally found in anti-cancer or anti-microbial peptides. They can be classified by origin (protein-derived, chimeric, or synthetic), physicochemical properties (hydrophilic, amphipathic, or hydrophobic), conformation (linear or cyclic), and type of cargo coupling (covalently or not non-covalently bound). Additionally, several modifications like cyclization, PEGylation and others can be introduced to improve their metabolic stability.<sup>55–59</sup>

CPPs' ability to pass through the cell membrane has been proven; however, the exact entry pathway remains poorly understood. Several mechanisms have been proposed for direct translocation, endocytosis, and endosomal escape, which seem to vary significantly and be sequence dependent, establishing another classification criteria.<sup>60–64</sup> Nanomedicine surface decoration with CPPs has been demonstrated to be an elegant N2B delivery approach to overcome the BBB.<sup>65–69</sup>

In one study, PEG-PLA polymeric micelles loaded with a blend of quercetin and etoposide were surface-modified with a potent CPP, RMMR1. This modification resulted in improved brain delivery efficiency and enhanced cellular uptake in glioblastoma (GBM) cells following IN administration. Notable tumor reduction and increased survival rates were achieved, with no significant changes in body weight. The CPP exhibited greater efficacy and significantly lower toxicity compared to the commonly used trans-activator of transcription (TAT) peptide.<sup>70</sup> Another CPP, DP7-C, was mixed with hyaluronic acid (HA) and siRNA to form a micellar structure HA/DP7-C. *In vitro* studies showed that this micelle had low cytotoxicity and improved cell uptake due to HA-CD44 interactions. *In vivo*, HA/DP7-C effectively delivered siRNA to the CNS *via* the trigeminal nerve pathway shortly after administration, enhancing accumulation at tumor sites. The intracellular delivery of anti-glioma siRNA inhibited tumor growth, increased survival time, and reduced tumor volume in GL261 tumor-bearing mice.<sup>71</sup>

Akita *et al.* (2021) studied the *in vitro* and *in vivo* functions of PAS-CPP (FFLIPKGRRRRRR) in facilitating the direct N2B transport of glucagon-like peptide 2 (GLP-2). Their findings showed that PAS-CPP-GLP-2 enhanced cellular uptake through macropinocytosis and promoted endosomal escape. Notably, IN administered PAS-CPP-GLP-2 produced an antidepressant effect within 20 minutes, achieving results comparable to intracerebroventricular (ICV) administration, while IV delivery did not.<sup>72</sup> A follow-up study qualitatively indicated that PAS-CPP-GLP-2 travels from the trigeminal nerve to the CNS *via* the principal sensory trigeminal nucleus and the trigeminal lemniscus. These results suggest that N2B delivery may occur through trigeminal axons as a transcellular pathway.<sup>73</sup>

However, there is contradictory evidence regarding the use of CPPs. When combined with liposomes, penetratin and TAT peptides did not improve insulin permeation across porcine nasal mucosa. In contrast, insulin-loaded liposomes that were not CPP-modified enhanced the nasal permeability coefficient, indicating that the system has the potential to optimize insulin absorption *via* the nasal route anyway without CPPs.<sup>74</sup>



## Mucus-modifying strategies

**Hyaluronidase.** As a permeation enhancer, hyaluronidase was utilized to improve the absorption of sEVs through the OR.<sup>75</sup> This enzyme loosens connective tissue by enzymatically cleaving components of the extracellular matrix (ECM). Specifically, hyaluronidase—regardless of whether it is derived from bacterial or vertebrate sources—catalyzes the hydrolysis of hyaluronic acid at the 1,4-glycosidic linkages.<sup>76</sup>

The use of brain-derived neurotrophic factor-loaded small extracellular vesicles (BDNF-sEVs) in stroke was investigated.<sup>77</sup> In a mouse model of ischemic stroke, IN administration was performed thirty minutes after delivering 10  $\mu$ L hyaluronidase (100 U per mouse). The sEVs were found to specifically target the *peri*-infarct region. This led to significantly improved efficacy, as evidenced by enhanced functional behavior, neural repair indicated by reduced infarct volume, increased neurogenesis and angiogenesis, improved synaptic plasticity, and fiber preservation, along with decreased expression of inflammatory cytokines and glial responses.<sup>77</sup>

**N-Acetylcysteine (NAC).** One example of a mucolytic compound with proven effects on reducing mucus viscosity and increasing clearance is NAC.<sup>78</sup> Hyaluronic acid/silk fibroin (HA/SF or HS) hydrogels, known for their sturdy mechanical properties, are staple biomaterials for tissue engineering. This study involved incorporating dopamine/polydopamine (DA/PDA) into HS hydrogels to create multifunctional HA/PDA/SF hydrogels aimed at N2B delivery. The mechanisms by which HDS/NAC hydrogels facilitate the opening of tight junctions in RPMI 2650 cells may be linked to inhibition of protein tyrosine phosphatase (PTP) due to the high mucin adhesion of NAC. In an *in vivo* imaging study (IVIS) conducted on rats, the amount of NAC delivered from the nasal cavity to brain tissue increased nearly nine-fold over 2 hours when using the HDS/NAC hydrogels, attributed to the photothermal response (PTR) effect induced by near-infrared (NIR) irradiation of the nasal tissue.<sup>79</sup>

In another study, Rao *et al.* (2024) developed a multifunctional nanocarrier system targeting the hypothalamic neurokinin receptor 3 (NK3R) through IN delivery. Utilizing a modified peptide, (Trp7,  $\beta$ -Ala8)-neurokinin A (4–10), conjugated with cysteine, the polymeric micelles containing the NK3R inhibitor SB222200 demonstrated effective hypothalamic cell uptake.<sup>80</sup> NAC was incorporated into the nanoparticles to enhance mucosal solubility and delivery efficacy. N2B delivery was then confirmed as an optimal method, minimizing the required oral dosage and sidesteps the BBB to target critical brain areas. *In vivo* studies on mouse newborn pups indicated that the system successfully targeted the hypothalamus and influenced NK3R-related functions in mice.<sup>80</sup>

## Protein-based nanoparticles

Protein-based nanoparticles (PNPs) are nanoscale carriers constructed primarily from natural or engineered proteins such as albumin, gelatin, silk fibroin, ferritin, or ovalbumin. They have emerged as promising platforms for the delivery of biologics, owing to their inherent biocompatibility, biodegradability, and

capacity for specific molecular interactions. Their overall safety makes them stand out from their synthetic polymers counterparts.<sup>81,82</sup>

Recent studies have demonstrated the structure, surface charge, and composition of PNPs that are critical for their performance in the nasal environment. Pho *et al.* (2022) systematically reviewed nasal absorption and the effect of protein corona in ovalbumin PNPs physico-chemical characteristics in porcine nasal mucus. The study concluded that zwitterionic, anionic, and cationic surface charges undergo rapid, moderate, and slow diffusion, respectively, as already observed in polymeric nanoparticles.<sup>83</sup>

Zwitterionic or neutral PNPs are generally more effective for traversing the nasal epithelium and achieving enhanced penetration into deeper tissues, including potential CNS access, while having limited nasal cavity retention time. In contrast, cationic PNPs tend to be retained within the mucus layer due to strong electrostatic interactions with negatively charged mucins. This retention can be advantageous for local immune system activation, making cationic PNPs particularly suitable for IN vaccination strategies.

**Small molecules and oligonucleotides.** Two recent studies reported the use of PNPs as carriers for N2B delivery in GBM therapy. Marrocco *et al.* (2024) utilized a stimuli-responsive ferritin-based PNP (The-0405) incorporating a topoisomerase 1 inhibitor (Genz-644282). In this approach, the PASE peptide was used to provide a stealth neutral surface, thereby decreasing non-specific interactions. Upon reaching the tumor microenvironment where matrix metalloproteases are overexpressed, the PASE shield is enzymatically cleaved, exposing the underlying ferritin surface, and unmasking its natural affinity for the transferrin receptor (TfR1/CD71) in both glioma cells and BBB. The PNP was administered IV and IN, the latter providing minimal distribution to peripheral organs such as the liver, kidney, and spleen as well as no signs of tissue damage or toxicity as demonstrated in histopathological analysis.<sup>84</sup>

On the other hand, Ha *et al.* (2021) developed a carrier-free, self-assembled NP system composed of two therapeutic molecules with opposite charges: antagonir-21, a negatively charged antisense oligonucleotide (ASO) targeting oncogenic miR-21, and RAGE-antagonist peptide (RAP), a positively charged peptide (net charge +9) derived from the RAGE-binding domain of HMGB-1. This system relied on a slight cationic surface and a particle size around 220 nm to facilitate N2B delivery.<sup>85</sup> Similar to the findings of Marrocco *et al.* (2024), the approach minimized systemic exposure and off-target effects, with nanoparticles primarily located in the brain. The treatment led to a marked reduction in tumor growth, decreased levels of the oncogenic miR-21, upregulation of pro-apoptotic genes, and inhibition of angiogenesis within the tumor.<sup>84</sup>

**Complex biologics and macromolecules.** The CNS delivery of large molecules has been severely limited by the restrictive nature of the BBB and the nasal epithelium, which was long thought to exclude macromolecules from effective N2B transport. However, recent advances have fundamentally challenged this paradigm. For example, Correa *et al.* (2023) has shown that repeated IN



administration of anti-Nogo-A monoclonal antibodies (mAbs) results in rapid and widespread distribution of the antibody throughout the brain and spinal cord, reaching CNS tissue concentrations comparable to those achieved by invasive intrathecal infusion. These antibodies cross the nasal epithelium, leading to significant functional recovery and neuroplasticity in preclinical models of stroke and neurodegeneration. Notably, the IN route achieves this with far less systemic exposure and without the need for traumatic procedures, marking a major advance in the non-invasive delivery of large biologics to the brain.<sup>86</sup>

The underlying mechanisms involve direct transport of Abs across the olfactory and trigeminal pathways, likely *via* transcytosis and facilitation by FcRn, which binds IgG at acidic endosomal pH and releases it at neutral pH on the opposite side of the epithelium. This mechanism allows Abs to reach deep brain regions and even the spinal cord, as confirmed by immunohistochemistry and functional studies. Additionally, FcRn's broad expression and its ability to protect IgG from degradation further enhance the efficiency and duration of therapeutic Ab presence in the CNS after nasal administration.<sup>87</sup>

### Biomimetic nanomedicines

Biomimetic nanomedicines mimic biological systems or structures, integrating natural cell membranes into their design to enhance specific functionalities and biocompatibility. These nanoparticles often consist of a synthetic core coated with cell membranes harvested from various cell types. This approach enhances their stability in circulation, improves targeting efficiency for drug delivery and reduces immune responses.<sup>88,89</sup> By leveraging the natural characteristics of cell membranes, they facilitate the tolerance of the local immune system for the nanomedicines, improving residence time and uptake, thus facilitating more effective therapeutic outcomes while minimizing adverse effects.

Reducing mutant huntingtin (mHTT) in the CNS *via* ASOs is a strategy currently undergoing clinical evaluation for Huntington's disease.<sup>90</sup> Aly *et al.* (2023) investigated the therapeutic potential of apolipoprotein A-I nanodisks (apoA-I NDs) as a delivery system for mHTT-lowering ASOs *via* the nasal route. After administration of apoA-I NDs in a BACHD transgenic mouse model, levels of apoA-I protein increased along the rostral-caudal brain axis, peaking in the rostral regions such as the OB and frontal cortex. Both apoA-I and ASOs were found in neurons. Notably, a single dose of apoA-I ASO-NDs significantly lowered mHTT levels in the brain areas most affected by Huntington's disease, specifically the cortex and striatum.<sup>91</sup>

A hypoxia-targeted carrier, RBP-Exo/AMO181a-chol, has been developed for delivering anti-microRNA-181a oligonucleotide to the brain, showing promise in stroke therapy. MicroRNA-181a (miR-181a) is usually elevated in ischemic brain tissue, and its suppression can mitigate ischemic damage. The exosome is engineered to bind to the receptor for advanced glycation end-products (RAGE), an overexpressed protein in hypoxic ischemic cells, through the incorporation of a RAGE-binding peptide (RBP-Exo). In a rat model of middle cerebral artery occlusion (MCAO), administration of RBP-Exo/

AMO181a-chol resulted in decreased levels of miR-181a and increased expression of Bcl-2. Furthermore, this treatment led to reduced tumor necrosis factor- $\alpha$  (TNF- $\alpha$ ) levels and apoptosis, significantly decreasing infarct size and providing neuroprotection in the ischemic brain compared to controls.<sup>92</sup>

Finally, N2B delivery of human umbilical cord mesenchymal stem cell exosomes (hUCMSC-Exos) demonstrated significant neuroprotective effects in PD mouse models by preventing dopaminergic neuron death in the substantia nigra pars compacta (SNpc). Treatment with hUCMSC-Exos notably enhanced locomotor abilities and increased the number of dopaminergic neurons in the SNpc. Additionally, it reduced glial activation and inflammatory responses in the OB and substantia nigra, improving the local microenvironment in PD mice. These results suggest that hUCMSC-Exos may restore olfactory and motor functions in mice with MPTP-induced PD, highlighting their potential as for clinical prevention and early treatment of PD.<sup>93</sup>

Overall, these findings suggest that particle size, volume, and charge, along with the utilization of enzymes, peptides, and additional enhancers, play a vital role in nanoparticle transport mechanisms for N2B delivery, offering opportunities to optimize drug delivery and enhance therapeutic outcomes. There are many existing research gaps within these improvement methods, especially in enzymes and enhancers for N2B nanoparticle delivery, as existing studies currently focus solely on nasal absorption.

## Experimental models of intranasal administration

To investigate the complexities of nasal drug delivery, especially in relation to membrane permeation and drug transport across the nasal epithelium, various *in vitro* and *ex vivo* models have been developed. These models serve as valuable alternatives to *in vivo* animal experimentation, enabling controlled studies on drug distribution, permeability, and cellular interactions.<sup>94</sup>

### *In vitro* models

*In vitro* cell models offer advantages such as high-throughput screening, precise control over experimental conditions, and mechanistic insight into drug transport.<sup>95,96</sup> A critical aspect in designing these models is replicating the nasal mucosal environment. This includes the use of natural nasal mucus, purified or recombinant mucins, and cellular components to mimic the dynamic and structural features of the nasal barrier.<sup>97</sup> The incorporation of *in vitro* cellular models introduces an additional aspect of directional permeability barrier consideration, giving researchers access to a variety of cell models for studying IN drug delivery. These include primary cell cultures, immortalized cell cultures, and commercially available alternative cell-type models. These models collectively contribute to our understanding of drug permeability and transport mechanisms across nasal barriers, which are critical for enhancing drug delivery efficiency.<sup>98</sup>



Primary cell cultures involve cultivating nasal epithelial cells isolated from human or animal donors. They retain native physiological characteristics, including tight junction formation and mucociliary differentiation. However, they are limited by donor variability, ethical concerns, short lifespan, and complex isolation procedures.<sup>99</sup>

Immortalized nasal cell lines such as RPMI 2650, Calu-3, 16HBE14o-, and Caco-2, are more accessible and reproducible, offering extended proliferation capacity and lower cost *versus* primary cultures. Traditionally cultured as monolayers in a single liquid environment, these cell lines have evolved into more advanced configurations, including air-liquid interface (ALI) models, which better simulate the semi-moist conditions of the nasal mucosa. These models have been extensively used to study drug transport and permeation through the nasal epithelium.<sup>98</sup>

In a study by Maaz *et al.* (2024), a PLGA nanoparticle formulation was administered using a pressurized metered dose inhaler (pMDI) and a three-dimensional (3D) human nasal cast model to evaluate deposition in the olfactory region.<sup>100</sup> Results indicated that direct aerosol exposure minimally impacted cell viability. Furthermore, aerosolized nanoparticles exhibited superior transport rates across the RPMI 2650 barrier compared to an aqueous nanoparticle suspension at all measured time intervals. This highlights the benefits of aerosol delivery and underscores the use of ALI cellular models in the evaluation of inhalable as opposed to simple solutions. The model not only sustains cells under ALI conditions but also allows for sampling from the basal chamber, making it suitable for assessing drug deposition, uptake, and transport kinetics in realistic environments.<sup>100</sup>

Commercially available alternative immortalized cell-type models have been employed in drug permeation studies to predict nasal drug delivery. One of the key models is the MucilAir® cell line, fully differentiated human nasal epithelium comprising basal, ciliated, and goblet cells. It forms a polarized barrier with well-established tight junctions, exhibiting active efflux properties *via* P-glycoprotein and BCRP transporters. MucilAir® has been validated for long-term cytotoxicity testing, mucus-drug interaction analysis, and studies of ciliary function.<sup>4,101</sup>

More advanced 3D co-culture systems integrate epithelial cells with immune or neuronal components to better reproduce the complexity of the nasal mucosa and its interactions with the CNS. These systems are particularly valuable for studying inflammatory responses, immune modulation, and neuronal uptake, although their higher complexity and cost limit widespread use. Similarly, mucosa-on-a-chip platforms that employ anatomy-based 3D printing and microfluidic technology recreate the dynamic environment of the nasal mucosa. These chips support ALI conditions, allow real-time observation of drug interactions, and facilitate modelling of inter-tissue crosstalk and mucin production, enhancing their physiological relevance.<sup>102,103</sup>

For these *in vitro* models, characterization of barrier and drug transport can be performed using transmission electron microscopy (TEM), also used for visualizing tight junctions and tracking nanoparticle uptake.<sup>104</sup> Furthermore, drug-

mucus interaction can be studied through both mechanical (*e.g.*, AFM, rheometry) and optical techniques. Optical methods such as dynamic light scattering (DLS), FT-IR, and Raman spectroscopy offer sensitive analysis of submicroscopic changes in mucus properties and protein corona formation around nanoparticles.<sup>105</sup> Fluorescence-based techniques, especially multi-particle tracking (MPT), enable direct visualization of nanoparticle mobility through mucus, providing quantitative insights into the diffusion behavior, and microviscosity of the nasal environment during drug delivery.<sup>106,107</sup>

### Ex vivo models

*Ex vivo* tissue models are also valuable tools for assessing N2B drug delivery. These models offer several advantages, including high tissue availability, direct isolation from human or experimental animal tissues, and the ability to obtain numerous tissue samples from a single subject, making them cost-effective and reproducible. However, their limitations include interindividual variability due to donor age, pathology, or diet, and a relatively short viability period.<sup>4</sup> Additionally, since the drug permeability of the olfactory epithelium in the nasal mucosa may be significantly higher than that of the respiratory mucosa, the selection of tissue source region should be consistent with the experimental objective, with this aspect difficult to control in *ex vivo* models.<sup>108</sup> Nasal inserts have emerged as a promising N2B delivery system, offering sustained drug release and improved brain targeting *via* the OR. In particular, rivastigmine tartrate-loaded nasal inserts were formulated using a gelatin/HPMC matrix through a quick-melting technique.<sup>109</sup> The inserts were comprehensively evaluated *ex vivo*, in which freshly isolated sheep olfactory nasal mucosa was used to investigate drug permeation, providing a physiologically relevant model. A custom-designed apparatus was also introduced to assess mucoadhesive strength under conditions simulating the nasal environment. This study highlights nasal inserts as a novel and effective strategy for enhancing CNS drug delivery, with *ex vivo* models playing a crucial role in validating both mucopermeation and mucoadhesion.

Understanding nasal drug deposition is critical for ensuring delivery to target regions, particularly the olfactory epithelium. Recent studies on thermosensitive *in situ* hydrogels containing rivastigmine-loaded lipid-based nanoparticles have shown promising results in enhancing drug retention and deposition in nasal tissues.<sup>110</sup>

A recent study analyzed the impact of tissue storage on the reliability of mucopermeation and mucoadhesion experiments using swine nasal mucosa.<sup>111</sup> The findings highlight the importance of appropriate tissue preparation to preserve mucosal integrity, which is essential for accurate assessment. Specifically, for Franz-type vertical diffusion assays, the use of freshly excised nasal mucosa is recommended. Storage of tissues at 4 °C or -20 °C was found to significantly overestimate drug permeability, potentially leading to misleading conclusions during formulation development. Histological analyses revealed that fresh tissues maintained intact epithelial architecture and preserved ultrastructure of adherens junc-



tions. In contrast, stored tissues exhibited disorganization, reduced mucosal thickness, and loss of epithelial integrity, all of which contributed to artificially elevated permeability. Therefore, the use of fresh mucosa is essential to ensure physiologically relevant and reproducible results.<sup>111</sup>

### In vivo models

*In vivo* models remain the most physiologically relevant approach for evaluating the PK and pharmacodynamics (PD) of N2B delivery. These models allow the exploration of the nasal mucosa in real time, including factors like mucosal congestion and nasal airflow, both of which significantly influence nanomedicine diffusion and deposition.<sup>105</sup> Indeed, formulation performance cannot be evaluated independently of the device used, since particle size distribution, spray plume geometry, actuation force, and dosing reproducibility vary between nasal sprays, inhalers, and micro-infusion systems, strongly influencing deposition patterns and brain targeting efficiency. Table 1 shows some strategies in nanomedicine formulation side-by-side with novel *in vivo* experimental models which will be discussed in this section. Among the most common *in vivo* analytical methods, hematological analysis, *e.g.*, measuring plasma or serum drug concentrations using HPLC, offers valuable insight into systemic BA following N2B

delivery.<sup>4</sup> Other techniques, such as *in situ* nasal perfusion, enable timed collection of nasal perfusate while preserving the animal's blood circulation and neural innervation. However, it is invasive, requiring surgical procedures and anesthesia, which limits throughput and adds experimental complexity.

To overcome the limitations of direct sampling, non-invasive imaging modalities such as magnetic resonance imaging (MRI), positron emission tomography (PET), and single-photon emission computed tomography (SPECT) are frequently used preclinically and clinically to study nanomedicine biodistribution. Optical fluorescence imaging (OFl) using NIR fluorophores reduces tissue scattering and absorption, facilitating clearer *in vivo* nasal imaging. Additionally, two-photon microscopy provides high-resolution imaging and deeper tissue penetration, enabling detailed assessment of nanomedicine interaction with the mucus layer and epithelial surfaces.<sup>112</sup>

The selection of animal models is essential for translational studies. Rats and mice are the most widely used due to their prominent olfactory epithelium, low cost, and standardized handling protocols, making them suitable for mechanistic research.<sup>113,114</sup> However, differences in nasal anatomy, dosing volumes, and brain size compared to humans limit their predictive value for clinical translation. Krishnan *et al.* (2017)

**Table 1** Highlighted *in vivo* nose-to-brain delivery studies in rodents using either innovative formulation strategies or avant-garde experimental models in the preclinical stage

Formulation strategy	Materials used	Experimental model	Main pharmacologic outcomes	Ref.
Mucoadhesive agents	Chitosan-modified transfersomes carrying insulin	STZ-induced neurodegeneration model in Wistar rats, treatment was administered by pipetting into nostril	Increased stability and mucosal uptake of insulin in nasal cavity; <i>in vivo</i> optical imaging showed longer residence time and controlled release in rat brain; enhanced neuroprotective effects	190
	Lyophilized nasal inserts made from HPMC and polycarbophil loaded with atomoxetine	Nasal inserts were administered <i>via</i> a PET tube to healthy Wistar rats	Improved brain-to-plasma concentration ratio of atomoxetine nasal insert vs oral and IP administration measured using LC-MS/MS	191
Mucopenetrative agents	Fluorescent liposomes of different surface charges with or without PEGylation	Esophageal reverse-intubation nasal administration in mice	Minimized variability of administered dose for more accurate PK analysis of N2B; neutral PEGylated liposomes had highest distribution in brain and spinal cord	52 and 122
	GLP-2 peptide derivative with R8 as CPP and FFLIPKG as penetration accelerating sequence (PAS)	ddY mice (depression model), treatment was administered by pipetting	PAS-CPP-GLP-2 migrates from the trigeminal nerve to the CNS through the principal sensory trigeminal nucleus and then through the trigeminal lemniscus; antidepressant effect comparable to ICV administration	72 and 73
Mucus-modifying agents	Polymeric NP loaded with NK3R antagonist and NAC	HFD-induced precocious puberty mouse model, treatment was administered by pipetting into nostril	Effective targeting of the hypothalamus, drug release, and amelioration of NK3R-related pubertal advancement	80
Protein-based nanoparticles	Function-blocking mAb 11C7 directed against the Nogo-A-specific region of rat Nogo-A	Long-Evans rats (photothrombotic stroke model), repeated treatment for 14 d administered by pipetting	All parts of the rat CNS (including spinal cord) were reached in therapeutic amounts, enhancing compensatory fiber sprouting and functional recovery after strokes, similar to intrathecal administration	86
	Anti-IL-1 $\beta$ Ab gel formed with Pluronic F127	LPS-induced neuroinflammation mouse model; <i>via</i> the MIND Technique (surgically implanted polymer-based material)	MIND delivery of anti-IL-1 $\beta$ significantly increased antibody diffusion through the CNS (measured by IVIS), leading to lower IL-1 $\beta$ levels compared to IV administration	125 and 126



observed that heavier and older Sprague-Dawley rats required increased IN doses to achieve the same brain concentrations as lighter and younger rats,<sup>115</sup> highlighting the importance of animal age and weight as experimental variables. Guinea pigs are particularly useful in immunological studies and tolerate moderate IN volumes (20–30  $\mu$ L),<sup>105</sup> but their nasal cavity structure diverges significantly from that of humans. Beagle dogs possess nasal structures and mucosal surface areas closer to humans, and they can be trained for repeated administrations, making them useful for PK and safety studies.<sup>98</sup> Nevertheless, their higher maintenance cost and ethical considerations limit widespread application. Non-human primates (NHPs), such as macaques, provide the closest anatomical and physiological resemblance to humans and thus the strongest translational value. They are particularly important for late-stage safety and efficacy studies. However, ethical constraints, logistical complexity, and cost restrict their use to select pre-clinical investigations.<sup>116</sup>

A persistent challenge in N2B drug development is accurately predicting regional deposition within the nasal cavity, which is difficult to achieve using *in vitro* or *ex vivo* methods alone. To address this gap, recent work<sup>117</sup> has focused on constructing anatomically realistic *in vitro* nasal cavity replicas (e.g., 3D-printed nasal casts) based on CT scans from adult human volunteers. These models capture inter-individual variability related to age and sex, resulting in 40 distinct nasal reconstructions that offer realistic airflow dynamics and structural fidelity. Such replicas have demonstrated superior predictive capacity for posterior deposition compared to traditional animal models, which, while valuable for toxicological and mechanistic studies, do not adequately replicate human nasal spray performance. Therefore, integrating data from both animal models and human-derived *in vitro* nasal replicas is crucial for improving the prediction of *in vivo* performance, particularly in the context of N2B delivery. The nasal casts allow for the evaluation of aerosol deposition patterns under realistic airflow conditions. When coupled with *in vitro* assays or cell-based inserts, they offer a robust platform for predicting drug behavior and optimizing formulations.<sup>118,119</sup>

Efforts to develop *in vitro*–*in vivo* correlations (IVIVC) for nasal delivery aim to predict drug deposition patterns and systemic absorption based on laboratory models. Although *in vitro* tools are widely employed to optimize formulation parameters and device performance, their predictive accuracy remains limited due to the anatomical complexity of the nasal cavity, variations in device-generated particle size and velocity, and patient-specific factors such as nasal airflow and mucosal conditions. Accordingly, IVIVC models that include device descriptors (e.g., D<sub>v</sub>50, plume angle, actuation profile) better capture deposition variability and translate more reliably to *in vivo* outcomes. Nevertheless, advances in *in vitro* modelling and improvements in *in vivo* imaging and sampling methods enable a deeper understanding of deposition mechanisms, which is expected to enhance IVIVC development. For example, Haasbroek-Pheiffer *et al.* (2023) reported preliminary extrapolations comparing fractional absorption in rodent

models with permeation across common epithelial cell lines such as Caco-2 and RPMI 2650, using compounds like atenolol, Acyclovir, methotrexate, and various tramadol nanoparticle formulations.<sup>4</sup>

The volume of nasal administration plays a key role in determining drug distribution and the extent of olfactory targeting. Studies have shown that low dosing volumes (e.g., 5  $\mu$ L in mice) help retain the drug within the nasal cavity, minimizing pulmonary exposure, whereas larger volumes ( $\geq 10$   $\mu$ L) may lead to deposition in the lungs.<sup>120</sup> In a study by Forero *et al.* (2022), various installation volumes (50–400  $\mu$ L) were tested in hamsters, revealing no major systemic differences compared to controls. However, histopathological analyses indicated inflammation in the lower respiratory tract in animals receiving 200 or 400  $\mu$ L, suggesting that higher volumes can result in aspiration of nasal or oropharyngeal contents and contribute to respiratory tract pathology.<sup>121</sup> Emerging techniques are also expanding the toolkit for evaluating N2B drug delivery. Reverse esophageal cannulation allows researchers to isolate and quantify drug transport *via* the olfactory route to the brain, minimizing systemic influence.<sup>122</sup>

Similarly, the minimally invasive nasal infusion (MINI) procedure offers precise delivery of protein therapeutics, such as ovalbumin, to the CNS with reduced procedural invasiveness and improved targeting accuracy. In this study, the use of a commercial microfluidic pump effectively facilitated the sustained delivery of proteins to different regions of the brain. MINI exhibited an efficiency of *ca.* 45% when compared to the ICV route. Furthermore, the pump's concentration, volume, and flow rate can be tailored to meet the requirements of specific therapeutic agents and applications. These results underscore the importance of targeting the olfactory mucosa to enhance the delivery of treatments to the CNS.<sup>123</sup> The MINI procedure is derived from the minimally invasive nasal depot (MIND) technique developed by Bleier *et al.*<sup>124–126</sup> which was designed to overcome dosing variability by direct delivery of the entire therapeutic dose to the olfactory submucosal space.

Finally, the safety profile of nasal DDS and devices must be carefully evaluated. Device design—spray nozzles, powder insufflators, nebulizers, or infusion pumps—directly influences mucosal deposition patterns, dosing reproducibility, and patient tolerability. Material compatibility, device geometry, and actuation mechanisms can affect mucosal integrity and local toxicity after administration. A recent overview highlights various health risks associated with nasal delivery devices, underscoring the need for biocompatible materials and robust preclinical safety assessments.<sup>127</sup>

## Translational insights from preclinical to clinical trials of nose-to-brain therapies: oxytocin and insulin

In the last three years, most ongoing clinical trials of N2B medications involve oxytocin and insulin. These stem from



their promising potential to address various neurological and psychiatric disorders. The trials also aim to leverage the unique delivery mechanisms that IN administration facilitates. In this section we focus on the clinical applications of two peptides as well as lessons learned from preclinical studies that might help achieve clinical approval of their nasal formulations.

### Oxytocin

Oxytocin is a neuropeptide hormone synthesized in the hypothalamus and released into the bloodstream by the pituitary gland. It plays crucial roles in various physiological processes, such as childbirth, lactation, and social bonding. Recent studies have emphasized its significant influence on social behaviors, emotional regulation, and psychological well-being.<sup>127</sup> Oxytocin IN has diverse clinical applications ranging from enhancing social interactions in autism spectrum disorder (ASD) and managing anxiety disorders to potential roles in pain management and neurodegenerative diseases. Its multifaceted effects on emotional and social processes mark it as a valuable therapeutic agent in various clinical contexts.

Clinical research indicates that IN oxytocin can improve social cognition and emotional recognition in individuals with ASD, enhancing communication and social engagement.<sup>128</sup> Oxytocin IN has also shown potential in mood disorders, for example, in reducing post-traumatic stress disorder (PTSD) symptoms by modulating stress responses and enhancing emotional processing.<sup>129</sup> However, further research is required to establish its definite effectiveness in this area. It is also associated with anxiolysis, reducing physiological reactions to stress and fostering better emotional regulation in anxious patients.<sup>130</sup> Other clinical applications include its use as an adjunct treatment for schizophrenia, where it may improve social cognition and emotional processing,<sup>128,131</sup> in chronic pain management, where it reduced pain severity<sup>132</sup> and in dementia, where it has shown tolerability and safety.<sup>133</sup>

However, current evidence suggests that IN oxytocin has not consistently met clinical efficacy endpoints across various trials. In a systematic review for its effectiveness against schizophrenia, studies have reported mixed or null results in improving negative symptoms,<sup>134</sup> while an RCT for Phelan-McDermid syndrome by Fastman *et al.* (2021) indicated variability in absorption and therapeutic effects.<sup>135</sup> Although some evidence suggests that nasal oxytocin may reach the brain in relevant amounts, these inconsistent outcomes imply that it has yet to demonstrate robust, reproducible benefits in clinical settings, despite the safety profile appearing generally favorable. Oxytocin disperses broadly throughout the brain rather than concentrating in areas that mediate its intended prosocial effects.<sup>136</sup> This wide dispersion may be influenced by challenges such as incomplete BBB crossing and variability in nasal passage uptake.<sup>137</sup> Consequently, the intended neuro-modulatory impact may be diluted, and factors like peripheral uptake or rapid clearance could further limit its central efficacy.

One strategy to improve brain BA of oxytocin is co-administration with vasoconstrictors. This method has worked with antidepressants, where vasoconstrictors reduced the absorption of the latter through the nasal vessels and increased its retention time in the nasal mucosa.<sup>138</sup> Another example, adrenaline, was co-administered with a castor oil-based gel matrix formulation of quinidine to male Wistar rats. Adrenaline can alter the absorption characteristics of P-glycoprotein substrate drugs such as quinidine by reducing nose-to-blood absorption, thereby allowing a greater amount of the drug to reach the brain *via* the nasal pathways.<sup>139</sup> A clinical study by Yao *et al.* (2023) demonstrated that the use of oxymetazoline pretreatment effectively reduced peripheral concentrations of IN oxytocin, enhancing its central effects without significantly increasing peripheral side effects.<sup>136</sup> This illustrates the potential benefits of utilizing vasoconstrictors to improve the targeted delivery of oxytocin *via* the nasal route.

New strategies to enhance N2B oxytocin delivery, especially through optimizing IN formulations, have gained traction. As mentioned earlier, enhancing the mucoadhesive properties of delivery systems can increase residence time in the nasal cavity, thereby facilitating better absorption and BA.<sup>140,141</sup> Using biodegradable polymers, such as chitosan or gelatin, to create oxytocin-carrying nanoparticles significantly improved the stability and encapsulation efficiency of the neuropeptide, ensuring more effective CNS delivery.<sup>141</sup> Another advanced strategy is the use of self-assembly of alkylated lysine-dendron oxytocin amphiphiles.<sup>142</sup> These dendritic structures enhanced peptide stability and sustained pharmacological activity. Their amphiphilic nature allows for effective self-aggregation in aqueous environments, leading to formation of nanostructures which can interface better with nasal mucosa. These amphiphiles can also form longer nanostrip structures, which may facilitate greater ligand interactions at the nanostrip-solvent interface compared to spherical structures. This enhanced interaction with oxytocin receptors suggests that self-assembled amphiphiles could provide a more efficient means of N2B oxytocin delivery, potentially improving therapeutic outcomes (Table 2).<sup>142</sup>

Employing the natural pathways for oxytocin delivery relies on leveraging the olfactory and trigeminal neural pathways to achieve a rapid reach to the brain. The use of IN sprays can effectively utilize these neural routes for more efficient CNS transport, evading first-pass metabolism.<sup>140</sup> Addressing inter-individual variability in response to oxytocin can also improve delivery strategies. Factors such as age, sex, and genetic predispositions may also affect response, which can be crucial when designing dosage regimens or individualized treatment protocols.<sup>128</sup>

These innovative strategies, including optimized formulation, leveraging natural neural pathways, and individualized treatment regimens, offer promising prospects for enhancing the N2B delivery of oxytocin and their combination may ultimately lead to its clinical translation.

### Insulin

Insulin is a peptide hormone produced by the pancreas, regulating glucose metabolism in the body. It facilitates glucose



**Table 2** Summary of strategies used in preclinical and clinical studies of intranasal oxytocin and insulin

Study type	Oxytocin	Insulin
Preclinical studies	Highlighted strategies: biodegradable polymers (chitosan or gelatin) to create oxytocin-carrying nanoparticles <sup>141</sup> and self-assembled of alkylated lysine-dendron oxytocin amphiphiles <sup>142</sup>	Highlighted strategies: co-delivery of insulin with protamine, <sup>155</sup> polysaccharide-peptide complexes stabilized around nanoemulsion droplets <sup>156</sup> administration by neonatal catheter for region-specific delivery either to olfactory or respiratory region <sup>157</sup>
Clinical studies	Clinical trials: Autism spectrum disorder, <sup>128</sup> post-traumatic stress disorder, <sup>129</sup> anxiety, <sup>130</sup> schizophrenia, <sup>128,131</sup> chronic pain, <sup>132</sup> and dementia <sup>133</sup> Strategy applied: co-administration with vasoconstrictor <sup>136</sup>	Clinical trials: Alzheimers disease, <sup>144,145</sup> delirium, <sup>146,147</sup> metabolic syndrome, <sup>148</sup> obesity (possible) <sup>149</sup> Strategy applied: nasal spray pumps <sup>158</sup>

uptake by cells, helping to maintain normal blood sugar levels. Insulin is essential for patients with diabetes, particularly those with Type 1 diabetes who cannot produce insulin naturally, and it also plays significant roles in various physiological and cognitive processes. N2B insulin presents diverse clinical applications, particularly in enhancing cognitive functions, managing postoperative complications, offering neuroprotection, and aiding metabolic health.

Nasal delivery of insulin offers advantages over other administration routes, as it has limited systemic distribution (approximately 3–8%), which reduces the risk of adverse reactions. In a study using a streptozocin (STZ)-induced rat model of neurodegeneration, which impairs cognition and memory while increasing A $\beta$  deposits, N2B insulin treatment resulted in improved learning and memory performance in the Morris water maze test. Treated rats also demonstrated enhanced swimming speed and distance compared to control rats.<sup>143</sup>

Insulin is also being studied for its potential to improve cognitive functions in individuals with AD and mild cognitive impairment (MCI). Clinical data indicates that it enhances memory performance and may counteract the effects of neurodegeneration by improving brain insulin signalling and glucose metabolism.<sup>144,145</sup> It has shown promise in reducing the incidence of postoperative delirium, particularly in elderly patients undergoing major surgery. Clinical studies indicate that insulin can decrease the prevalence of delirium and regulate biomarkers associated with neuroinflammation.<sup>146,147</sup> Interestingly, emerging evidence suggests that N2B insulin may also aid in treating olfactory dysfunction.

Insulin is most relevant in the treatment of metabolic disorders. Its IN administration improves metabolic dysfunction and insulin resistance, enabling better glucose control with lower risk of hypoglycemia. This approach is beneficial for patients with Type 2 diabetes or metabolic syndrome who struggle with conventional insulin therapies.<sup>148</sup> It has also been investigated for its effects on appetite regulation. Some trials indicate that it reduces food intake and influences reward pathways in the brain, suggesting possible applications in obesity management.<sup>149</sup>

However, several issues limit nasal insulin effectiveness. One key problem is its low BA; due to its hydrophilicity and its vulnerability to enzymes in the nasal cavity, only a fraction of the dose reaches the brain in rats unless formulations are optimized with permeation enhancers.<sup>150</sup> While it has shown

promise in early clinical trials by improving cognition in patients with MCI and AD,<sup>151,152</sup> more recent trials have reported inconsistent outcomes, with some studies indicating no significant slowing of cognitive decline.<sup>153</sup> Although insulin is safe and potentially effective in certain subpopulations, the overall clinical results are mixed, and its efficacy has not been universally established.<sup>144</sup> Furthermore, there is a potential risk of hypoglycemia at high doses, which underscores the need for carefully optimized dosing protocols, as evidenced by a phase I clinical study.<sup>154</sup>

Preclinical strategies described earlier for improving insulin delivery may solve these clinical limitations. In particular, a study by Wu *et al.* (2023) involving co-delivery of insulin with protamine seems feasible for clinical applications, since protamine is also FDA-approved.<sup>155</sup> Another paper involves the development of polysaccharide-peptide complexes stabilized around nanoemulsion droplets, which has shown promise for nasal delivery of insulin and pramlintide.<sup>156</sup> The nanoparticles maintain stability in physiological conditions while enhancing their mucosal penetration, utilizing both passive diffusion and endocytic uptake mechanisms. The controlled release profile afforded is another advantage, allowing for sustained delivery, potentially reducing administration frequency, which is beneficial for chronic conditions requiring consistent management such as diabetes and neurodegenerative disorders.<sup>156</sup>

Another strategy is using region-specific nasal administration either to the OR or RR. This method was demonstrated by Maigler *et al.* (2021), where they administered a small volume (2.5  $\mu$ l) of insulin detemir to C57BL/6 mice using a neonatal catheter and Hamilton syringe.<sup>157</sup> This technique was developed using a 3D nasal cast made from CT scans of murine skulls. The region-specific administration was carried out by introducing the catheter 8 mm into the mouse nostril for OR targeting and while it was introduced only 2 mm deep for RR targeting. Peripheral bioactivity was then measured using a glucose tolerance test where RR-administered insulin detemir showed higher peripheral distribution compared to that which was OR-administered. However, both methods still showed significantly less distribution to the periphery compared to SC-administered insulin detemir.<sup>157</sup> This novel method caters to the significant avoidance of adverse risk reactions such as hypoglycemia by careful delivery to the specific nasal cavity region.



On the clinical side, three nasal pump-actuator designs were evaluated for delivering a 400 IU mL<sup>-1</sup> insulin solution by analyzing droplet size distribution, plume geometry, spray pattern, and *in vitro* deposition in a nasal cast.<sup>158</sup> The design with the best spray characteristics for N2B delivery (spray angle of 30° to 45°; droplet size of 20 to 50 µm) enhanced deposition in the nasal cast and was used in a pharmacological MRI study in healthy male volunteers. Functional MRI revealed statistical reductions in regional cerebral blood flow in insulin receptor-rich areas (bilateral amygdala) after N2B administration of insulin (160 IU) *versus* saline control. These findings align with the anticipated impact of insulin on the brain and were achieved with a straightforward nasal spray device and formulation.<sup>158</sup>

Recent advancements in N2B insulin formulation and administration, particularly through innovative strategies discussed above, hold considerable potential for enhancing its therapeutic efficacy in neurological conditions. Continued exploration here will be pivotal for translating these findings into clinical practice, ultimately benefiting conditions where both metabolic and neurological regulations are compromised.

## Regulatory hurdles in translation of nose-to-brain therapies

The development of N2B nanomedicines for clinical use encounters significant regulatory hurdles, particularly concerning safety and efficacy validation. Key challenges include demonstrating appropriate drug absorption through the nasal mucosa, minimizing systemic side effects, and ensuring effective drug deposition in target areas of the brain.<sup>159,160</sup> For instance, FDA-approved nasal products exemplify successful entries into the market, showcasing that IN delivery systems are already used in treating several CNS conditions (Table 3).<sup>161–168</sup> However, achieving widespread clinical application remains contingent upon overcoming the specific barriers for N2B delivery mechanisms and ensuring consistent patient outcomes. Possible solutions that contribute to overcoming these regulatory challenges include local toxicology studies such as mucosal irritation and nasal histopathology

observations, as well as systemic ones such as neurobehavioral testing.<sup>169</sup> In addition, measurement of neuroinflammatory markers would ensure that the formulation is not causing untoward CNS inflammation.<sup>170</sup> In terms of the medical devices to be used, it is important to consider the relevant ISO standards early in the development, such as ISO 13485, ISO 20072, and ISO 27427.<sup>171,172</sup> Incorporating pharmaceutical quality systems (ICH Q8-Q10) even at the start of basic studies would be beneficial especially if the end goal is clinical translation, ensuring that product development is both scientific and systematic.<sup>173,174</sup>

Meanwhile, the Cuban NeuroEPO (NeuralCIM®) is an IN-administered, neuroprotective, low-sialic-acid variant of recombinant human erythropoietin (EPO) produced by the Center of Molecular Immunology (CIM/CIMAB). Preclinically, NeuroEPO was found to be transported *via* multiple potentially periocular and mucosal routes, including olfactory and trigeminal pathways, CSF circulation, and vascular routes. It did not damage the respiratory mucosa and was well-tolerated in short-term nasal administration in rats.<sup>175,176</sup> NeuralCIM® has been approved as a clinical treatment for AD, by the Cuban Regulatory Authority (CECMED).<sup>177</sup> The ATHENEAE RCT evaluated mild-to-moderate AD patients. Safety endpoints included hematologic parameters to confirm a lack of hematopoietic activity, as well as nasal tolerability and adverse event profiles. Efficacy endpoints in AD cohorts encompassed cognitive scales, quality of life measures, and general neuropsychological batteries to detect signals of cognitive benefit and reported safety.<sup>178,179</sup> NeuralCIM® has not received formal approval outside Cuba, but its development's rigorous efficacy and safety design could serve as a model for meeting regulatory requirements.

## Expert opinion and future perspectives

Selective brain delivery while avoiding peripheral exposure is critical for certain biomolecules, insulin being the most classical example as we discussed above. Additionally, the brain plays a vital role in regulating peripheral insulin sensitivity.<sup>180</sup> Consequently, researchers have explored brain-specific delivery methods for insulin, including nanomedicine-based

**Table 3** US FDA-approved intranasal medications with clinical indications for CNS conditions according to the FDA website (<https://dps.fda.gov/medguide>; <https://www.accessdata.fda.gov/scripts/cder/daf/index.cfm>)

Drug	Dosage form	Manufacturing company	Clinical indications	Approval year	Ref.
Nafarelin acetate (Synarel®)	Metered spray	Pfizer	Central precocious puberty (gonadotropin-dependent precocious puberty) in children	1990	161
Nalmefene (Opree®)	Spray	Indiovor	Opioid overdose emergency treatment	1995	162
Midazolam (Nayzilam®)	Spray	UCB Inc	Epilepsy in children and adults	2019	163
Diazepam (Valtoco®)	Spray	Neurelis Inc	Epilepsy in children and adults	2020	164
Dihydroergotamine mesylate (Trudhesa™)	Metered spray	Impel Neuropharma	Migraine in adults	2021	165
Zavegeptan (Zavzpret™)	Metered spray	Pfizer	Migraine in adults	2023	166
Dihydroergotamine (Atzumi™)	Powder	Satsuma Pharmaceuticals	Migraine in adults	2025	167
Esketamine hydrochloride (Spravato®)	Spray	Janssen Pharm	Depression in adults	2025	168



approaches, which have been the focus of various comprehensive review articles.<sup>145</sup>

Again, selective inhibition of enzymes such as carnitine palmitoyl transferase 1A (CPT1A) in the hypothalamus—without affecting peripheral tissues—demonstrates the benefits of delivering biomolecules like CPT1A inhibitors specifically to the brain.<sup>181</sup> This approach minimizes peripheral exposure and serves as a valuable example of brain-targeted delivery for managing metabolic disorders related to energy balance disruption. We used a core-crosslinked polymeric micelle-type nanomedicine platform allowing efficient delivery of a specific CPT1A inhibitor that modifies brain lipid metabolism using ICV.<sup>182,183</sup> Acknowledging ICV as an invasive brain administration option, specifically for life-style related pathological conditions such as obesity and diabetes, we began to explore non-invasive delivery options, such as the IN route.

Despite its advantages of being non-invasive, patient-friendly, and effective technique for CNS drug delivery, several factors hinder its effectiveness, including low nasal mucosal permeability, the presence of proteases, and mucociliary clearance (Fig. 3). In this work, we have outlined the beneficial effects of both mucoadhesive and mucopenetrative strategies. Existing literature on *in vivo* results shows that neither of the two systems outperforms the other.<sup>184</sup> The outcomes can vary depending on factors such as the disease model, the targeted area of the brain, and the therapeutics used. Investigating the combination of mucoadhesive with mucopenetrative functions in an optimal ratio within the same nanomedicine platform could also be valuable.

For example, See *et al.* (2020) developed a liquid crystal (LC) formulation consisting of C<sub>17</sub>-monoglycerol ester (MGE) and Pluronic® F-127 for the N2B delivery of tranilast, a lipophilic

### Improvements in Experimental models

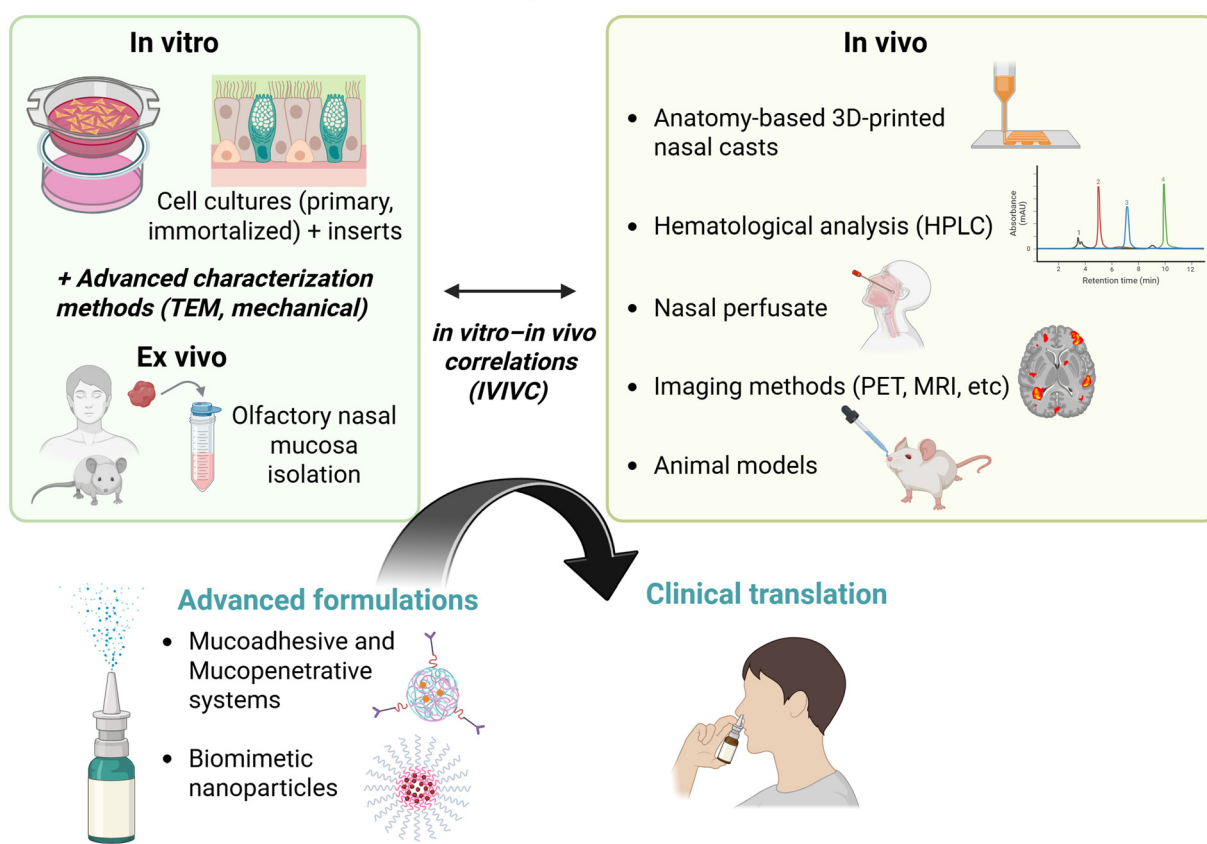


**Fig. 3** Schematic overview of recent advancements in nose-to-brain (N2B) drug delivery research, spanning from *in vitro* and *in vivo* models to clinical applications. A range of *in vitro* and *ex vivo* systems have been developed to investigate the complexities of nasal drug delivery, particularly regarding membrane permeation and drug transport across the nasal epithelium. These models enable controlled, high-throughput studies, offering precise experimental control and mechanistic insights when combined with advanced optical and mechanical characterization techniques. *In vivo* models remain the most physiologically relevant approach for evaluating the pharmacokinetics and pharmacodynamics of N2B delivery. Tools such as *in situ* nasal perfusion, non-invasive imaging, animal models, and anatomically accurate 3D-printed nasal casts derived from human CT scans provide valuable platforms with predictive capabilities. Efforts to establish *in vitro*–*in vivo* correlations (IVIVC) are ongoing, aiming to bridge laboratory findings with real-world drug deposition and absorption. Concurrently, significant progress has been made in developing advanced IN formulations, including mucoadhesive, mucopenetrative, and nanoparticle-based systems optimized for N2B delivery. These technological and methodological advances are enabling the clinical translation of promising IN therapies—such as those based on oxytocin and insulin—by enhancing formulation strategies and our understanding of delivery mechanisms.



drug.<sup>185</sup> An H2 inverted hexagonal phase LC was formed, which exhibited longer residence time in the nasal cavity and higher brain-to-plasma concentration compared to a non-LC control, which is similar in mechanism to mucoadhesive formulations. However, when ethanol was added to the LC, plasma  $C_{\text{max}}$  and AUC increased *ca.* 10-fold to that of the original formulation. The authors hypothesized that effective dissolution of tranilast in ethanol in combination with the membrane permeation enhancer effect of MGE, as well as increased formulation viscosity, may have favored drug absorption in the respiratory epithelium rather than in the olfactory epithelium.<sup>185</sup> This further highlights the need to study the interplay between mucoadhesive and mucopenetrative properties of different formulation components.

Furthermore, it is essential to establish a method for selecting the ideal drug carriers for mucosal delivery tailored to the specific payload and therapeutic target. Gao *et al.* (2023) conducted molecular dynamics (MD) simulations to analyze the all-atom dynamic characteristics of interactions between various delivery systems, focusing on their mucoadhesive and mucopenetrative properties, as well as their interaction with the nasal mucus protein MUC5AC.<sup>186</sup> They compared their findings with experimental data from *in vitro* and *ex vivo* mucosal penetration studies using four different nanoparticle types. The authors claimed that there was a valid correlation between the material properties predicted by MD simulations and the delivery performance of the nanoparticles. These insights into their molecular mechanisms with different physicochemical properties may provide valuable information for screening and optimizing nanomaterials suitable for nasal delivery.

It is also critical to recognize that the biochemical nature of the nasal mucosa—including the amount of mucin, mucus turnover rate, and water movement within the mucus—can vary between species, individuals, and even within the same individual. For example, factors such as age, health conditions, the presence of inflammatory molecules, or even the surrounding environment can alter mucus function, ultimately affecting transmucosal drug delivery.<sup>187</sup> Given these various factors, utilizing artificial intelligence (AI) and machine learning (ML) for optimal material design may be a practical approach provided that these variables are accounted for when designing materials, planning experiments, interpreting the results, and, most importantly, during translating laboratory findings to the clinic.

We discussed the challenges associated with dosing volume in the context of IN drug delivery in previous sections, along with the issues related to mucociliary clearance, which significantly limits the exposure time of active compounds. One approach to address this limitation is to choose therapeutics with high pharmacological potency and specificity, particularly those that exhibit nanomolar to picomolar potency. Potent molecules can allow for the administration of smaller absolute doses, potentially enhancing therapeutic effectiveness despite rapid clearance. In the field of nanomedicine, advanced formulations that utilize specific materials or sophisticated nano-

structures can improve drug delivery by achieving very high drug loading capacities while maintaining stability and viscosity, both crucial for effective delivery. Implementing sustained release mechanisms or designing systems that respond to pathological stimuli—such as pH, glutathione, or temperature variations—can further enhance therapeutic effects by prolonging drug release at the targeted site. Additionally, developing innovative IN delivery devices capable of accurately dispensing multiple micro-doses over extended periods—from minutes to hours—could improve the patient experience. These devices can be designed to deliver medication comfortably, potentially increasing the cumulative dose that targets the upper nasal cavity and optimizing therapeutic outcomes. However, to fully realize the potential of IN delivery, it is essential to simultaneously address current challenges related to material design and formulations, as well as advanced delivery tools. This involves developing specialized spraying devices that can improve drug residence time, creating biocompatible nasal inserts with controlled release mechanisms, and designing depot-forming gels with predictable degradability. Establishing a robust communication framework between specialists in materials design and device design is crucial in this process. By fostering an environment where professionals from both fields can actively collaborate, it is possible to ensure that their respective processes align and enhance one another. This collaboration allows materials experts to share insights into the characteristics and performance of new materials, whereas device designers can provide feedback on how these materials perform in practical applications. This synergistic relationship leads to the optimization of both materials and devices, ultimately resulting in innovative solutions that meet the challenges of N2B delivery.

In addition, results obtained from rodent models may not always translate to higher species as expected. We have previously discussed the anatomical differences in the nasal cavity between rodents and other mammals. A recent paper expressed scepticism about the positive PK results from IN administration in rodents reported by a significant number of previous publications. Driedonks *et al.* (2022) highlighted that the results from higher species, such as pig-tailed macaques (*Macaca nemestrina*), may not be as optimistic.<sup>188</sup> In this study, the authors examined the PK and biodistribution of Expi293F-derived EVs labelled with a nanoluciferase reporter (palmGRET) in pig-tailed macaques, comparing IV and IN administration over a 125-fold dose range. The results indicated that the N2B delivery of EVs was minimal in macaques and suggested that the EVs may be retained in the nasal cavity, preventing their distribution to other areas. Further investigation revealed significant nanoluciferase activity in the nasal lavage fluid, with very strong signals compared to the signals observed in both simultaneously collected plasma and CSF.<sup>188</sup>

The authors also noted that the discrepancy between previously published data reporting high brain delivery of EVs *via* the IN route and their findings of low brain distribution may be due to the different sources of the EVs and the brain disease models used. For example, models of brain injury



(such as tumors, stroke, and morphine treatment) may enhance the uptake of EVs compared to healthy animals. Although IN delivery of EVs to the brain was not more efficient than IV, the systemic exposure to peripheral organs such as the lungs, liver, and spleen was still minimal with this route.<sup>188</sup> This confirms that N2B delivery is the preferred alternative in cases where systemic exposure may lead to off-target effects.

On the other hand, a study by Sasaki *et al.* (2023) uncovered more optimistic results using NHP models.<sup>189</sup> The authors devised a combined system for N2B delivery which includes a unique mucoadhesive powder formulation (drug substance with the microcrystalline cellulose-containing Ceolus®) alongside a specifically designed nasal device termed the “N2B-system”. They then assessed the biodistribution of two model drugs Texas Red-labelled dextran<sub>3000</sub> (TR-DEX) and domperidone. Their data on “N2B-system” efficacy showed a significantly higher distribution ratio of the formulations within the OR, as evidenced by both an *in vitro* study utilizing a 3D nasal cast and *in vivo* experiments conducted with cynomolgus monkeys (*Macaca fascicularis*). This contrasted favorably with alternative nasal DDS, which primarily consisted of a proprietary nasal powder device aimed at enhancing nasal absorption and vaccination, as well as a commercially available liquid spray.<sup>189</sup>

Taken together, these findings underscore the novelty of our review in highlighting how mechanistic nanomedicine strategies, informed by experimental models and translational insights, can directly improve N2B delivery. By integrating recent technological advancements, careful nanomedicine design, and translational considerations, researchers can overcome current challenges in N2B delivery and enhance the clinical effectiveness of CNS-targeted therapeutics (Fig. 3). This comprehensive perspective, linking mechanistic strategies to translational applications, represents a unique contribution of this review.

## Author contributions

Conceptualization: W. K. P., S. Q., and R. R.-R.; visualization: P. M. H., S. Q., and R. R.-R.; writing – original draft: W. K. P., C. P. R., P. M. H., C. A. G., P. A. G.-P., S. Z., S. Q., and R. R.-R.; language editing – P. M. H.; writing – review and editing: W. K. P., S. Q., and R. R.-R.

## Conflicts of interest

There are no conflicts to declare.

## Data availability

No primary research results, software or code have been included, and no new data were generated or analysed as part of this review.

## Acknowledgements

W. K. P. is supported by the Beatriu de Pinós Programme (2023 BP 00247) coordinated by the Agència de Gestió d'Àjuts Universitaris i de Recerca (AGAUR), Generalitat de Catalunya. S. Q. is financially supported by Japan Science and Technology Agency (JST) funded the open innovation platform for industry-academia co-creation (COI-NEXT) Program (Grant Number JPMJPF2202). R. R.-R. is supported by the Ministerio de Ciencia, Innovación y Universidades, Agencia Estatal de Investigación (AEI; PID2023-146716OB-I00) and by AGAUR, Generalitat de Catalunya (Producte, PROD 00094).

## References

- 1 E. Taha, A. Shetta, S. A. Nour, M. J. Naguib and W. Mamdouh, *Mol. Pharm.*, 2024, **21**(3), 999–1014.
- 2 J. Wang, Y. Zhang, M. Zhang, S. Sun, Y. Zhong, L. Han, Y. Xu, D. Wan, J. Zhang and H. Zhu, *Drug Des., Dev. Ther.*, 2022, **16**, 279–296.
- 3 F. Laffleur and B. Bauer, *Int. J. Pharm.*, 2021, **607**, 120994.
- 4 A. Haasbroek-Pheiffer, S. Van Niekerk, F. Van Der Kooy, T. Cloete, J. Steenekamp and J. Hamman, *Biopharm. Drug Dispos.*, 2023, **44**, 94–112.
- 5 S. Nakhaee, F. Saeedi and O. Mehrpour, *Heliyon*, 2023, **9**(12), e23083.
- 6 T. P. Crowe, M. H. W. Greenlee, A. G. Kanthasamy and W. H. Hsu, *Life Sci.*, 2018, **195**, 44–52.
- 7 F. Moradi and N. Dashti, *Naunyn-Schmiedeberg's Arch. Pharmacol.*, 2022, **395**, 133–148.
- 8 E. M. Olsson, P. A. Lönnqvist, C. O. Stiller, S. Eksborg and S. Lundeberg, *Pediatr. Anesth.*, 2021, **31**(6), 631–636.
- 9 A. Inglewicz and R. K. Szymczak, *Pharmaceutics*, 2024, **16**, 519.
- 10 M. M. Messeha and G. Z. El-Morsy, *Anesth. Essays Res.*, 2018, **12**(1), 170–175.
- 11 A. Anno, R. Djagbletey, P. Sarpong, E. Aniteye, E. Lamptey, G. Aryee, R. Essuman, E. O. Darkwa and A. Quarshie, *Open Access Maced. J. Med. Sci.*, 2023, **11**, 184–190.
- 12 K. Xu, S. Duan, W. Wang, Q. Ouyang, F. Qin, P. Guo, J. Hou, Z. He, W. Wei and M. Qin, *Wiley Interdiscip. Rev.: Nanomed. Nanobiotechnol.*, 2024, **16**(2), e1956.
- 13 A. K. Singh, A. Singh and N. V. S. Madhv, *J. Drug Delivery Ther.*, 2012, **2**(3), DOI: [10.22270/jddt.v2i3.163](https://doi.org/10.22270/jddt.v2i3.163).
- 14 D. Mittal, A. Ali, S. Md, S. Baboota, J. K. Sahni and J. Ali, *Drug Deliv.*, 2014, **21**(2), 75–86.
- 15 V. S. P. Sudheer and K. Shetty, *Pharm. Sci. Asia*, 2023, **50**, 175–186.
- 16 M. L. Formica, D. A. Real, M. L. Picchio, E. Catlin, R. F. Donnelly and A. J. Paredes, *Appl. Mater. Today*, 2022, **29**, 101631.
- 17 R. D. Alvites, A. R. Caseiro, S. S. Pedrosa, M. E. Branquinho, A. S. P. Varejão and A. C. Maurício, *Anat. Rec.*, 2018, **301**, 1678–1689.



18 M. N. Pereira, C. Venâncio, M. D. L. Pinto, S. Alves-Pimenta and B. Colaço, *Lab. Anim.*, 2024, **58**, 324–333.

19 A. W. Barrios, G. Núñez, P. Sánchez Quinteiro and I. Salazar, *Front. Neuroanat.*, 2014, **8**, 63.

20 N. J. Johnson, L. R. Hanson and W. H. I. Frey, *Mol. Pharm.*, 2010, **7**, 884–893.

21 I. N. Pérez-Osorio, A. Espinosa, M. Giraldo Velázquez, P. Padilla, B. Bárcena, G. Fragoso, H. Jung-Cook, H. Besedovsky, G. Meneses and E. L. Sciuotto Conde, *J. Pharmacol. Exp. Ther.*, 2021, **378**, 244–250.

22 W. A. Banks, J. E. Morley, M. L. Niehoff and C. Mattern, *J. Drug Targeting*, 2009, **17**, 91–97.

23 M. B. Chauhan and N. B. Chauhan, *J. Neurol. Neurosurg.*, 2015, **2**, 009.

24 S. Yadav, F. Gattacceca, R. Panicucci and M. M. Amiji, *Mol. Pharm.*, 2015, **12**, 1523–1533.

25 A. M. Tolomeo, G. Zuccolotto, R. Malvicini, G. De Lazzari, A. Penna, C. Franco, F. Caicci, F. Magarotto, S. Quarta, M. Pozzobon, A. Rosato, M. Muraca and F. Collino, *Pharmaceutics*, 2023, **15**, 548.

26 K. Phukan, M. Nandy, R. B. Sharma and H. K. Sharma, *Recent Pat. Drug Delivery Formulation*, 2016, **10**, 156–164.

27 R. Raliya, D. Saha, T. S. Chadha, B. Raman and P. Biswas, *Sci. Rep.*, 2017, **7**, 44718.

28 S. Quader, K. Kataoka and H. Cabral, *Adv. Drug Delivery Rev.*, 2022, **182**, 114115.

29 E. Marcello and V. Chiono, *Int. J. Mol. Sci.*, 2023, **24**, 3390.

30 M. R. Knowles and R. C. Boucher, *J. Clin. Invest.*, 2002, **109**, 571–577.

31 L. Cui, Y. Yang, Y. Hao, H. Zhao, Y. Zhang, T. Wu and X. Song, *Clin. Rev. Allergy Immunol.*, 2025, **68**, 12.

32 M. Boegh and H. M. Nielsen, *Basic Clin. Pharmacol. Toxicol.*, 2015, **116**, 179–186.

33 B. Poinard, S. Kamaluddin, A. Q. Q. Tan, K. G. Neoh and J. C. Y. Kah, *ACS Appl. Mater. Interfaces*, 2019, **11**, 4777–4789.

34 T. L. Carlson, J. Y. Lock and R. L. Carrier, *Annu. Rev. Biomed. Eng.*, 2018, **20**, 197–220.

35 A. A. Date, G. Halpert, T. Babu, J. Ortiz, P. Kanvinde, P. Dimitrion, J. Narayan, H. Zierden, K. Betageri, O. Musmanno, A. A. Wiegand, X. Huang, S. Gumber, J. Hanes and L. M. Ensign, *Biomaterials*, 2018, **185**, 97–105.

36 R. Pathak, R. Prasad Dash, M. Misra and M. Nivsarkar, *Acta Pharm. Sin. B*, 2014, **4**, 151–160.

37 R. Phongpradist, J. Jiaranaikulwanitch, K. Thongkorn, S. Lekawanijit, S. Sirilun, C. Chittasupho and W. Poomanee, *Gels*, 2023, **9**, 610.

38 H. A. Abo El-Enin, R. E. Mostafa, M. F. Ahmed, I. A. Naguib, M. A. Abdelgawad, M. M. Ghoneim and E. M. Abdou, *Pharmaceutics*, 2022, **14**, 410.

39 M. V. G. Botan, J. B. da Silva and M. L. Bruschi, *AAPS PharmSciTech*, 2024, **25**, 258.

40 A. Alshweiat, I. Csóka, F. Tömösi, T. Janáky, A. Kovács, R. Gáspár, A. Sztojkov-Ivanov, E. Ducza, Á. Márki, P. Szabó-Révész and R. Ambrus, *Int. J. Pharm.*, 2020, **579**, 119166.

41 S. Cunha, C. P. Costa, J. A. Loureiro, J. Alves, A. F. Peixoto, B. Forbes, J. M. Sousa Lobo and A. C. Silva, *Pharmaceutics*, 2020, **12**, 599.

42 A. Giuliani, A. G. Balducci, E. Zironi, G. Colombo, F. Bortolotti, L. Lorenzini, V. Galligioni, G. Pagliuca, A. Scagliarini, L. Calzà and F. Sonvico, *Drug Delivery*, 2018, **25**, 376–387.

43 D. G. Gadhave, M. Quadros, A. R. Ugale, M. Goyal, S. Ayehunie and V. Gupta, *Int. J. Biol. Macromol.*, 2024, **267**, 131491.

44 C. Madsen, *Brain Behav.*, 2017, **7**(6), e00696.

45 L. F. González, E. Acuña, G. Arellano, P. Morales, P. Sotomayor, F. Oyarzun-Ampuero and R. Naves, *J. Controlled Release*, 2021, **331**, 443–459.

46 H. Zhang, Y. Chen, M. Yu, Y. Xi, G. Han, Y. Jin, G. Wang, X. Sun, J. Zhou and Y. Ding, *Proc. Natl. Acad. Sci. U. S. A.*, 2023, **120**, e2304213120.

47 P. C. Pires, A. C. Fazendeiro, M. Rodrigues, G. Alves and A. O. Santos, *Eur. J. Pharm. Sci.*, 2021, **164**, 105918.

48 Y. Lu, J. T.-W. Wang, N. Li, X. Zhu, Y. Li, S. Bansal, Y. Wang and K. T. Al-Jamal, *J. Controlled Release*, 2023, **359**, 257–267.

49 L. R. Michels, F. N. S. Fachel, R. S. Schuh, J. H. Azambuja, P. O. de Souza, N. E. Gelsleichter, G. S. Lenz, F. Visioli, E. Braganhol and H. F. Teixeira, *J. Controlled Release*, 2023, **355**, 343–357.

50 S. A. Kumbhar, C. R. Kokare, B. Shrivastava, B. Gorain and H. Choudhury, *J. Pharm. Sci.*, 2021, **110**, 1761–1778.

51 N. Subhash Hinge, H. Kathuria and M. Monohar Pandey, *Eur. J. Pharm. Biopharm.*, 2023, **190**, 131–149.

52 T. Kurano, T. Kanazawa, A. Ooba, Y. Masuyama, N. Maruhana, M. Yamada, S. Iioka, H. Ibaraki, Y. Kosuge, H. Kondo and T. Suzuki, *J. Controlled Release*, 2022, **344**, 225–234.

53 M. Wang, Y. Lv, H. Xu, X. Zhao, G. Zhang, S. Wang, C. Wang, W. Wu, L. Wu, W. Zhu and J. Zhang, *Carbohydr. Polym.*, 2025, **348**, 122881.

54 S. Ruan, J. Li, H. Ruan, Q. Xia, X. Hou, Z. Wang, T. Guo, C. Zhu, N. Feng and Y. Zhang, *J. Controlled Release*, 2024, **366**, 712–731.

55 M. Green and P. M. Loewenstein, *Cell*, 1988, **55**, 1179–1188.

56 M. Zorko and Ü. Langel, *Adv. Drug Delivery Rev.*, 2005, **57**, 529–545.

57 P. Järver and Ü. Langel, *Biochim. Biophys. Acta, Biomembr.*, 2006, **1758**, 260–263.

58 V. P. Torchilin, *Pept. Sci.*, 2008, **90**, 604–610.

59 I. Szabó, M. Yousef, D. Soltész, C. Bató, G. Mező and Z. Bánóczi, *Pharmaceutics*, 2022, **14**, 907.

60 S. El-Andaloussi, T. Holm and U. Langel, *Curr. Pharm. Des.*, 2005, **11**, 3597–3611.

61 F. Madani, S. Lindberg, Ü. Langel, S. Futaki and A. Gräslund, *J. Biophys.*, 2011, **2011**, 414729.

62 E. Trofimenko, G. Grasso, M. Heulot, N. Chevalier, M. A. Deriu, G. Dubuis, Y. Arribat, M. Serulla, S. Michel, G. Vantomme, F. Ory, L. C. Dam, J. Puyal, F. Amati,



A. Lüthi, A. Danani and C. Widmann, *eLife*, 2021, **10**, e69832.

63 E. Trofimenko, Y. Homma, M. Fukuda and C. Widmann, *Cell Rep.*, 2021, **37**, 109945.

64 M. Serulla, P. Anees, A. Hallaj, E. Trofimenko, T. Kalia, Y. Krishnan and C. Widmann, *Eur. J. Pharm. Biopharm.*, 2023, **184**, 116–124.

65 T. Kanazawa, F. Akiyama, S. Kakizaki, Y. Takashima and Y. Seta, *Biomaterials*, 2013, **34**, 9220–9226.

66 T. Kanazawa, T. Kurano, H. Ibaraki, Y. Takashima, T. Suzuki and Y. Seta, *Pharmaceutics*, 2019, **11**, 478.

67 T. Kanazawa, H. Taki and H. Okada, *Eur. J. Pharm. Biopharm.*, 2020, **152**, 85–94.

68 Y. Zhang, P. Guo, Z. Ma, P. Lu, D. Kebebe and Z. Liu, *J. Nanobiotechnol.*, 2021, **19**, 255.

69 J. Maeng and K. Lee, *Front. Pharmacol.*, 2022, **13**, 1068495.

70 J. Koo, Y. Shin, H. Jeon, J. Cheong, S. Cho, C. Park, E. C. Song, J. D. Ramsey, C. Lim and K. T. Oh, *J. Controlled Release*, 2025, **378**, 997–1012.

71 Y. Yang, X. Zhang, S. Wu, R. Zhang, B. Zhou, X. Zhang, L. Tang, Y. Tian, K. Men and L. Yang, *J. Controlled Release*, 2022, **342**, 66–80.

72 T. Akita, R. Kimura, S. Akaguma, M. Nagai, Y. Nakao, M. Tsugane, H. Suzuki, J.-I. Oka and C. Yamashita, *J. Controlled Release*, 2021, **335**, 575–583.

73 T. Akita, Y. Oda, R. Kimura, M. Nagai, A. Tezuka, M. Shimamura, K. Washizu, J.-I. Oka and C. Yamashita, *J. Controlled Release*, 2022, **351**, 573–580.

74 E. de Souza Von Zuben, J. O. Eloy, V. H. S. Araujo, M. P. D. Gremião and M. Chorilli, *Colloids Surf. A*, 2021, **622**, 126624.

75 W. Shen, T. You, W. Xu, Y. Xie, Y. Wang and M. Cui, *Pharmaceutics*, 2023, **15**, 2578.

76 A. I. Petkova, I. Kubajewska, A. Vaideanu, A. G. Schätzlein and I. F. Uchegbu, *Pharmaceutics*, 2022, **14**, 1136.

77 X. Zhou, X. Deng, M. Liu, M. He, W. Long, Z. Xu, K. Zhang, T. Liu, K.-F. So, Q.-L. Fu and L. Zhou, *J. Controlled Release*, 2023, **357**, 1–19.

78 P. Rogliani, G. M. Manzetti, S. Gholamalishahi, M. Cazzola and L. Calzetta, *Int. J. Chronic Obstruct. Pulm. Dis.*, 2024, **19**, 2347–2360.

79 T.-W. Chung, C.-L. Cheng, Y.-H. Liu, Y.-C. Huang, W.-P. Chen, A. K. Panda and W.-L. Chen, *Biomater. Adv.*, 2023, **154**, 213615.

80 Q. Rao, Y. Xu, X. Wang, H. Luo, H. Li, J. Xiong, H. Gao and G. Cheng, *SusMat*, 2024, **4**, e222.

81 S. Hong, D. W. Choi, H. N. Kim, C. G. Park, W. Lee and H. H. Park, *Pharmaceutics*, 2020, **12**, 604.

82 D. Verma, N. Gulati, S. Kaul, S. Mukherjee and U. Nagaich, *J. Pharm.*, 2018, **2018**, 9285854.

83 T. Pho and J. A. Champion, *ACS Appl. Mater. Interfaces*, 2022, **14**, 51697–51710.

84 F. Marrocco, E. Falvo, L. Mosca, G. Tisci, A. Arcovito, A. Reccagni, C. Limatola, R. Bernardini, P. Ceci, G. D'Alessandro and G. Colotti, *Cell Death Dis.*, 2024, **15**, 1–10.

85 J. Ha, M. Kim, Y. Lee and M. Lee, *Nanoscale*, 2021, **13**, 14745–14759.

86 D. Correa, M. I. Scheuber, H. Shan, O. W. Weinmann, Y. A. Baumgartner, A. Harten, A.-S. Wahl, K. L. Skaar and M. E. Schwab, *Proc. Natl. Acad. Sci. U. S. A.*, 2023, **120**, e2200057120.

87 M. Fieux, S. Le Quellec, S. Bartier, A. Coste, B. Louis, C. Giroudon, M. Nourredine and E. Bequignon, *Int. J. Mol. Sci.*, 2021, **22**, 6475.

88 T. Jiang, Y. Zhan, J. Ding, Z. Song, Y. Zhang, J. Li and T. Su, *ChemMedChem*, 2024, **19**(22), e202400410.

89 Y. Wu, S. Wan, S. Yang, H. Hu, C. Zhang, J. Lai, J. Zhou, W. Chen, X. Tang, J. Luo, X. Zhou, L. Yu, L. Wang, A. Wu, Q. Fan and J. Wu, *J. Nanobiotechnol.*, 2022, **20**(1), 542.

90 M. E. Rook and A. L. Southwell, *BioDrugs*, 2022, **36**, 105–119.

91 A. E.-E. Aly, N. S. Caron, H. F. Black, M. E. Schmidt, C. Anderson, S. Ko, H. J. E. Baddeley, L. Anderson, L. L. Casal, R. S. M. Rahavi, D. D. O. Martin and M. R. Hayden, *J. Controlled Release*, 2023, **360**, 913–927.

92 M. Kim, Y. Lee and M. Lee, *Nanoscale*, 2021, **13**, 14166–14178.

93 W. Huang, T. Zhang, X. Li, L. Gong, Y. Zhang, C. Luan, Q. Shan, X. Gu and L. Zhao, *Neuroscience*, 2024, **549**, 1–12.

94 A. Wengst and S. Reichl, *Eur. J. Pharm. Biopharm.*, 2010, **74**, 290–297.

95 F. Sousa and P. Castro, in *Concepts and Models for Drug Permeability Studies*, ed. B. Sarmento, Woodhead Publishing, 2016, pp. 83–100.

96 C. Mercier, E. Jacqueroux, Z. He, S. Hodin, S. Constant, N. Perek, D. Boudard and X. Delavenne, *Eur. J. Pharm. Biopharm.*, 2019, **139**, 186–196.

97 M. Yang, S. K. Lai, Y.-Y. Wang, W. Zhong, C. Happe, M. Zhang, J. Fu and J. Hanes, *Angew. Chem., Int. Ed.*, 2011, **50**, 2597–2600.

98 R. Boyuklieva, P. Zagorchev and B. Pilicheva, *Biomedicines*, 2023, **11**, 2198.

99 V. Manna and S. Caradonna, *STAR Protoc.*, 2021, **2**, 100782.

100 A. Maaz, I. S. Blagbrough and P. A. De Bank, *Mol. Pharm.*, 2024, **21**, 1108–1124.

101 P. J. Callaghan, B. Ferrick, E. Rybakovsky, S. Thomas and J. M. Mullin, *Biosci. Rep.*, 2020, **40**, BSR20201532.

102 M. Usman Khan, X. Cai, Z. Shen, T. Mekonnen, A. Kourmatzis, S. Cheng and H. Gholizadeh, *Pharmaceutics*, 2023, **15**, 1557.

103 S. Bendas, E. V. Koch, K. Nehlsen, T. May, A. Dietzel and S. Reichl, *Pharmaceutics*, 2023, **15**, 2245.

104 D. Ye, K. A. Dawson and I. Lynch, *Analyst*, 2014, **140**, 83–97.

105 T. Hua, S. Li and B. Han, *Expert Opin. Drug Delivery*, 2024, **21**, 553–572.

106 J. A. McGlynn, N. Wu and K. M. Schultz, *J. Appl. Phys.*, 2020, **127**, 201101.

107 C. S. Schneider, Q. Xu, N. J. Boylan, J. Chisholm, B. C. Tang, B. S. Schuster, A. Henning, L. M. Ensign,



E. Lee, P. Adstamongkonkul, B. W. Simons, S.-Y. S. Wang, X. Gong, T. Yu, M. P. Boyle, J. S. Suk and J. Hanes, *Sci. Adv.*, 2017, **3**, e1601556.

108 P. Berben, A. Bauer-Brandl, M. Brandl, B. Faller, G. E. Flaten, A.-C. Jacobsen, J. Brouwers and P. Augustijns, *Eur. J. Pharm. Sci.*, 2018, **119**, 219–233.

109 L. Shaghilil, A. Alshishani, A. A. Sa'aleek, H. Abdelkader and Y. Al-ebini, *J. Drug Delivery Sci. Technol.*, 2022, **76**, 103736.

110 C. P. Costa, J. N. Moreira, J. M. Sousa Lobo and A. C. Silva, *Acta Pharm. Sin. B*, 2021, **11**, 925–940.

111 J. S. M. de Araújo, G. G. X. Augusto, A. M. Pestana, F. C. Groppo, F. S. M. Rodrigues, P. D. Novaes and M. Franz-Montan, *AAPS PharmSciTech*, 2024, **26**, 7.

112 N. Geva-Zatorsky, D. Alvarez, J. E. Hudak, N. C. Reading, D. Erturk-Hasdemir, S. Dasgupta, U. H. von Andrian and D. L. Kasper, *Nat. Med.*, 2015, **21**, 1091–1100.

113 M. C. Veronesi, M. Alhamami, S. B. Miedema, Y. Yun, M. Ruiz-Cardozo and M. W. Vannier, *Am. J. Nucl. Med. Mol. Imaging*, 2020, **10**, 1–31.

114 H. Shen, N. Aggarwal, B. Cui, G. W. Foo, Y. He, S. K. Srivastava, S. Li, M. Z. X. Seah, K. S. Wun, H. Ling, I. Y. Hwang, C. L. Ho, Y. S. Lee and M. W. Chang, *Cell*, 2025, **188**, 1545–1562.

115 J. K. S. Krishnan, P. Arun, B. Chembukave, A. P. Appu, N. Vijayakumar, J. R. Moffett, N. Puthillathu and A. M. A. Namboodiri, *J. Neurosci. Methods*, 2017, **286**, 16–21.

116 M. E. Emborg, *ILAR J.*, 2007, **48**, 339–355.

117 A. Alfaifi, S. Hosseini, A. R. Esmaeili, R. Walenga, A. Babiskin, T. Schuman, W. Longest, M. Hindle and L. Golshahi, *Int. J. Pharm.*, 2022, **622**, 121858.

118 L. Deruyver, C. Rigaut, P. Lambert, B. Haut and J. Goole, *Adv. Drug Delivery Rev.*, 2021, **175**, 113826.

119 C. Rigaut, L. Deruyver, M. Niesen, M. Vander Ghinst, J. Goole, P. Lambert and B. Haut, *Pharmaceutics*, 2023, **15**, 2661.

120 D. S. Southam, M. Dolovich, P. M. O'Byrne and M. D. Inman, *Am. J. Physiol.: Lung Cell. Mol. Physiol.*, 2002, **282**, L833–L839.

121 C. Forero, J. M. Ritter, J. N. Seixas, J. D. Coleman-McCrory, M. Brake, J. A. Condrey, C. Tansey, S. R. Welch, S. C. Genzer and J. R. Spengler, *Pathogens*, 2022, **11**(8), 898.

122 M. Fukuda, T. Kanazawa, S. Iioka, T. Oguma, R. Iwasa, S. Masuoka, N. Suzuki, Y. Kosuge and T. Suzuki, *J. Controlled Release*, 2021, **332**, 493–501.

123 V. Di Francesco, A. J. Chua, E. Davoudi, J. Kim, B. S. Bleier and M. M. Amiji, *J. Controlled Release*, 2024, **372**, 674–681.

124 S. Padmakumar, G. Jones, G. Pawar, O. Khorkova, J. Hsiao, J. Kim, M. M. Amiji and B. S. Bleier, *J. Controlled Release*, 2021, **331**, 176–186.

125 V. Di Francesco, A. J. Chua, B. S. Bleier and M. M. Amiji, *ACS Appl. Mater. Interfaces*, 2024, **16**, 69103–69113.

126 A. J. Chua, V. Di Francesco, A. D'Souza, M. Amiji and B. S. Bleier, *Lab. Anim.*, 2024, **53**, 363–375.

127 D. Ishii, M. Kageyama and S. Umeda, *PLoS One*, 2021, **16**, e0261451.

128 D. Martins, M. Paduraru and Y. Paloyelis, *Br. J. Pharmacol.*, 2021, **179**, 1525–1543.

129 S. K. Houlton, J. G. Vaidya, P. Breheny and L. Strathearn, *Res. Sq. [Preprint]*, 2024, rs.3.rs-3912105, DOI: [10.21203/rs.3.rs-3912105/v1](https://doi.org/10.21203/rs.3.rs-3912105/v1).

130 M. M. E. Riem, L. E. Kunst, M. H. J. Bekker, M. Fallon and N. Kupper, *Psychoneuroendocrinology*, 2020, **111**, 104482.

131 D. Martins, C. Davies, A. D. Micheli, D. Oliver, A. Krawczun-Rygmaczewska, P. Fusar-Poli and Y. Paloyelis, *Transl. Psychiatry*, 2020, **10**, 227.

132 M. Flynn, T. S. Campbell, M. Robert, M. Nasr-Esfahani and J. A. Rash, *Internet J. Gynecol. Obstet.*, 2020, **152**, 425–432.

133 A. S. Sawares, J. Olver, M. Morcos and T. R. Norman, *Australas. Psychiatry*, 2024, **33**, 33–44.

134 M. Sabe, N. Zhao, A. Crippa, G. P. Strauss and S. Kaiser, *Int. J. Neuropsychopharmacol.*, 2021, **24**, 601–614.

135 J. Fastman, J. Foss-Feig, Y. Frank, D. Halpern, H. Harony-Nicolas, C. Layton, S. Sandin, P. Siper, L. Tang, P. Trelles, J. Zweifach, J. D. Buxbaum and A. Kolevzon, *Mol. Autism*, 2021, **12**, 62.

136 S. Yao, Y. Chen, Q. Zhuang, Y. Zhang, C. Lan, S. Zhu, B. Becker and K. M. Kendrick, *Mol. Psychiatry*, 2023, **28**, 3083–3091.

137 S. Yao and K. M. Kendrick, *Pharmaceutics*, 2022, **14**, 323.

138 Z. Jin, Y. Han, D. Zhang, Z. Li, Y. Jing, B. Hu and S. Sun, *Pharmaceutics*, 2022, **14**, 2070.

139 L. A. Bors, Á. Bajza, M. Mándoki, B. J. Tasi, G. Cserey, T. Imre, P. Szabó and F. Erdő, *Brain Res. Bull.*, 2020, **160**, 65–73.

140 D. S. Quintana, A. Lischke, S. Grace, D. Scheele, Y. Ma and B. Becker, *Mol. Psychiatry*, 2021, **26**, 80–91.

141 M. C. Selles, J. T. S. Fortuna, Y. P. R. de Faria, L. D. Siqueira, R. Lima-Filho, B. M. Longo, R. C. Froemke, M. V. Chao and S. T. Ferreira, *iScience*, 2023, **26**(4), 106545.

142 F. Xie, Y. Lin, Å. Andersson, I. Vetter, L. Zhao and J. Wan, *Chem. Commun.*, 2023, **59**, 13855–13858.

143 F. Nojoki, B. Ebrahimi-Hosseini, A. Hatamian-Zarmi, F. Khodagholi and K. Khezri, *Biomed. Pharmacother.*, 2022, **153**, 113450.

144 S. Craft, R. Raman, T. W. Chow, M. S. Rafii, C. Sun, R. A. Rissman, M. Donohue, J. B. Brewer, C. Jenkins, K. Harless, D. Gessert and P. Aisen, *JAMA Neurol*, 2020, **77**, 1099.

145 C. Y. Wong, A. Baldelli, C. M. Hoyos, O. Tietz, H. X. Ong and D. Traini, *Drug Delivery Transl. Res.*, 2024, **14**, 1776–1793.

146 Y. Mi, L. Zhou, L. Ge, X. Liu, W. Ouyang, X. Chang and X. He, *Drug Des. Devel. Ther.*, 2025, **19**, 759–769.

147 Y. Nakadate, M. Yamada, N. Kusuyama, R. Ishii, H. Sato, T. Schricker and M. Tanaka, *Trials*, 2023, **24**(1), 822.

148 N. Torabi, M. Nazar, J. Fahanik-Babaei and A. Eliassi, *Physiol. Pharmacol.*, 2020, **24**, 268–275.



149 J. Wingrove, O. O'Daly, A. D. L. Rubio, S. A. Hill, M. Swedroska, B. Forbes, S. A. Amiel and F. Zeloya, *Hum. Brain Mapp.*, 2022, **43**, 5432–5451.

150 H.-D. Bae, J. S. Lee, H. Pyun, M. Kim and K. Lee, *Drug Delivery*, 2019, **26**, 622–628.

151 H. B. Schiöth, W. H. Frey, S. Brooks and J. C. Benedict, *Expert Rev. Clin. Pharmacol.*, 2012, **5**, 17–20.

152 A. Claxton, L. D. Baker, C. W. Wilkinson, E. H. Tritschuh, D. Chapman, G. S. Watson, B. Cholerton, S. R. Plymate, M. Arbuckle and S. Craft, *J. Alzheimer's Dis.*, 2013, **35**, 789–797.

153 A. Woodfield, T. Gonzales, E. Helmerhorst, S. Laws, P. Newsholme, T. Porter and G. Verdile, *Int. J. Mol. Sci.*, 2022, **23**, 15811.

154 F. F. Schmitzberger, J. Fowler, C. H. Hsu, M. Pai, R. W. Neumar, W. J. Meurer and R. Silbergleit, *Circulation*, 2022, **146**, A105–A105.

155 J. Wu, N. Jones, N. A. L. Fayed, P.-H. Chao, A. Wu, D. R. de Araujo, E. Rouhollahi, A. Jia and S.-D. Li, *J. Controlled Release*, 2023, **356**, 373–385.

156 C. Zuglianello, N. G. M. Silva and E. Lemos-Senna, *J. Drug Delivery Sci. Technol.*, 2023, **85**, 104527.

157 F. Maigler, S. Ladel, J. Flamm, S. Gänger, B. Kurpiers, S. Kiderlen, R. Völk, C. Hamp, S. Hartung, S. Spiegel, A. Soleimanizadeh, K. Eberle, R. Hermann, L. Krainer, C. Pitzer and K. Schindowski, *Pharmaceutics*, 2021, **13**, 1904.

158 J. Wingrove, M. Swedrowska, R. Scherließ, M. Parry, M. Ramjeeawon, D. Taylor, G. Gauthier, L. Brown, S. Amiel, F. Zeloya and B. Forbes, *J. Controlled Release*, 2019, **302**, 140–147.

159 L.-A. Keller, O. Merkel and A. Popp, *Drug Delivery Transl. Res.*, 2022, **12**, 735–757.

160 A. Ghosh, A. Majie, V. Karmakar, K. Chatterjee, S. Chakraborty, M. Pandey, N. Jain, S. Roy Sarkar, A. B. Nair and B. Gorain, *AAPS PharmSciTech*, 2024, **25**, 96.

161 Pfizer, Synarel® (nafarelin acetate) nasal solution Medication Guide, [https://www.accessdata.fda.gov/drugsatfda\\_docs/label/2023/019886s039lbl.pdf#page=28](https://www.accessdata.fda.gov/drugsatfda_docs/label/2023/019886s039lbl.pdf#page=28), (accessed July 23, 2025).

162 Indiovor, OPVEE® (nalmefene) nasal spray prescribing information, [https://www.accessdata.fda.gov/drugsatfda\\_docs/label/2023/217470Orig1s000.pdf](https://www.accessdata.fda.gov/drugsatfda_docs/label/2023/217470Orig1s000.pdf), (accessed October 12, 2025).

163 UCB Inc, NAYZILAM® (midazolam) nasal spray Medication Guide, [https://www.accessdata.fda.gov/drugsatfda\\_docs/label/2023/211321s008lbl.pdf#page=26](https://www.accessdata.fda.gov/drugsatfda_docs/label/2023/211321s008lbl.pdf#page=26), (accessed July 23, 2025).

164 Neurelis Inc, VALTOCO® (diazepam nasal spray) Medication Guide, [https://www.accessdata.fda.gov/drugsatfda\\_docs/label/2023/211635s008lbl.pdf#page=24](https://www.accessdata.fda.gov/drugsatfda_docs/label/2023/211635s008lbl.pdf#page=24), (accessed July 23, 2025).

165 Impel Neuropharma, TRUDHESATM (dihydroergotamine mesylate) nasal spray Medication Guide, [https://www.accessdata.fda.gov/drugsatfda\\_docs/label/2021/213436s000lbl.pdf#page=22](https://www.accessdata.fda.gov/drugsatfda_docs/label/2021/213436s000lbl.pdf#page=22), (accessed July 23, 2025).

166 Pfizer, ZAVZPRETTM (zavegeptan) nasal spray prescribing information, [https://www.accessdata.fda.gov/drugsatfda\\_docs/label/2025/216386s007lbl.pdf](https://www.accessdata.fda.gov/drugsatfda_docs/label/2025/216386s007lbl.pdf), (accessed October 12, 2025).

167 Satsuma Pharmaceuticals, ATZUMITM (dihydroergotamine) nasal powder Medication Guide, [https://www.accessdata.fda.gov/drugsatfda\\_docs/label/2025/217901s000lbl.pdf#page=19](https://www.accessdata.fda.gov/drugsatfda_docs/label/2025/217901s000lbl.pdf#page=19), (accessed July 23, 2025).

168 Janssen Pharms, SPRAVATO® ( esketamine) nasal spray Medication Guide, [https://www.accessdata.fda.gov/drugsatfda\\_docs/label/2025/211243s016lbl.pdf#page=47](https://www.accessdata.fda.gov/drugsatfda_docs/label/2025/211243s016lbl.pdf#page=47), (accessed July 23, 2025).

169 I. Drath, F. Richter and M. Feja, *Transl. Neurodegener.*, 2025, **14**, 23.

170 M. Feja, I. Drath, S. Weiß, A. Ewe, B. Gericke, T. F. Outeiro, L. Stefanis, A. Aigner and F. Richter, *Mol. Ther. – Nucleic Acids*, 2025, **36**(3), 102671.

171 O. Nerbrink and J. P. Mitchell, *J. Aerosol Med. Pulm. Drug Delivery*, 2012, **25**, 209–216.

172 P. W. J. Linders, *Biomed. Instrum. Technol.*, 2020, **54**, 68–70.

173 N. A. Charoo and A. A. Ali, *Drug Dev. Ind. Pharm.*, 2013, **39**, 947–960.

174 C. Aaberg, H. Dahmen, C. Davies, P. L. Sandau and R. Srinivasan, *PDA J. Pharm. Sci. Technol.*, 2021, **75**, 188–206.

175 K. Suárez, G. Fernández, G. P. Seguí, C. L. Pérez and Y. R. Cruz, *Rev haban cienc méd*, 2022, **21**(5), e5061.

176 K. S. Borras, G. F. Peña, G. P. Seguí, Y. R. Cruz and C. P. Hernández, *Rev haban cienc méd*, 2022, **21**(4), e4849.

177 L. Pérez, S. S. Pérez, T. R. Obaya, N. U. Amable, C. V. Silva, C. E. V. González and K. L. Monzón, *Alzheimers Dement.*, 2023, **19**, e071685.

178 L. Pérez, S. Sosa, G. Bringas, D. López, C. Valenzuela, A. I. Peñalver, E. Dalmau, T. Rodríguez and N. Urrutia, *Alzheimers Dement.*, 2020, **16**, e036167.

179 S. Sosa, G. Bringas, N. Urrutia, A. I. Peñalver, D. López, E. G. Dalmau, A. Fernández, Z. M. Hernández, A. Vina-Rodríguez, Y. Peña, J. F. Batista, C. Valenzuela, K. León, T. Crombet, T. Rodríguez, L. Pérez, Y. Álvarez, M. C. G. Rodríguez, N. Vázquez, M. Rodríguez, Y. González, M. A. Ramos, Y. López, M. A. B. Hernández, L. Madruga, D. Carmona, J. E. Acosta, M. López, D. Amaro, O. L. Baños, M. O. Álvarez, A. T. Cordero, M. Betancourt, L. Padrón, E. R. Chavez, I. García, Y. Morgan, M. Charles, M. González, M. D. L. C. Rodríguez, Y. León, J. M. López, Y. Acosta, T. Virués, L. Pérez, K. León-Arcia, R. Periche, A. Valero, Y. C. Pozo, G. Horta, R. Quesada, E. Luz, L. Torres, S. Romero, M. E. Rodríguez and D. Estévez, *Alzheimer Res. Ther.*, 2023, **15**(1), 215.

180 J. L. Milstein and H. A. Ferris, *Mol. Metab.*, 2021, **52**, 101234.

181 R. Rodríguez-Rodríguez, M. Baena, S. Zagmutt, W. K. Paraiso, A. C. Reguera, R. Fadó and N. Casals, *Pharmacol. Rev.*, 2025, **7**(3), 100051.



182 W. K. D. Paraiso, J. Garcia-Chica, X. Ariza, S. Zagmunt, S. Fukushima, J. G. Gomez, Y. Mochida, D. Serra, L. Herrero, H. Kinoh, N. Casals, K. Kataoka, R. Rodriguez-Rodriguez and S. Quader, *Biomater. Sci.*, 2021, **9**, 7076–7091.

183 J. Garcia-Chica, W. K. D. Paraiso, S. Zagmunt, A. Fosch, A. C. Reguera, S. Alzina, L. Sánchez-García, S. Fukushima, K. Toh, N. Casals, D. Serra, L. Herrero, J. Garcia, K. Kataoka, X. Ariza, S. Quader and R. Rodríguez-Rodríguez, *Biomater. Sci.*, 2023, **11**, 2336–2347.

184 K. Netsomboon and A. Bernkop-Schnürch, *Eur. J. Pharm. Biopharm.*, 2016, **98**, 76–89.

185 G. L. See, F. Arce, S. Dahlizar, A. Okada, M. F. B. M. Fadli, I. Hijikuro, S. Itakura, M. Katakura, H. Todo and K. Sugibayashi, *J. Controlled Release*, 2020, **325**, 1–9.

186 X. Gao, Y. Xiong, H. Chen, X. Gao, J. Dai, Y. Zhang, W. Zou, Y. Gao, Z. Jiang and B. Han, *J. Controlled Release*, 2023, **353**, 366–379.

187 J. Leal, H. D. C. Smyth and D. Ghosh, *Int. J. Pharm.*, 2017, **532**, 555–572.

188 T. Driedonks, L. Jiang, B. Carlson, Z. Han, G. Liu, S. E. Queen, E. N. Shirk, O. Gololobova, Z. Liao, L. H. Nyberg, G. Lima, L. Paniushkina, M. Garcia-Contreras, K. Schonvisky, N. Castell, M. Stover, S. Guerrero-Martin, R. Richardson, B. Smith, V. Mahairaki, C. P. Lai, J. M. Izzi, E. K. Hutchinson, K. A. M. Pate and K. W. Witwer, *J. Extracell. Biol.*, 2022, **1**, e59.

189 K. Sasaki, S. Fukakusa, Y. Torikai, C. Suzuki, I. Sonohata, T. Kawahata, Y. Magata, K. Kawai and S. Haruta, *J. Controlled Release*, 2023, **359**, 384–399.

190 F. Nojoki, B. Ebrahimi-Hosseinzadeh, A. Hatamian-Zarmi, F. Khodagholi and K. Khezri, *Biomed. Pharmacother.*, 2022, **153**, 113450.

191 M. H. Teaima, M. T. El-Nadi, R. R. Hamed, M. A. El-Nabarawi and R. Abdelmonem, *Pharmaceuticals*, 2023, **16**, 326.

